Diamagnetism and neutrals depletion in a plasma

A. Fruchtman[1] and S. Shinohara[2]

[1]*Department of Physics, Faculty of Sciences,*

H. I. T. - Holon Institute of Technology,

52 Golomb Street, Holon 58102, Israel and

[2]*Division of Advanced Mechanical Systems Engineering,*

Institute of Engineering, Tokyo University of Agriculture and Technology,

2-24-16, Naka-cho, Koganei, Tokyo 184-8588, Japan

(Dated: September 26, 2017)

Abstract

Recent experimental and theoretical findings [Physics of Plasmas 23, 122108 (2016)] regarding the pressure balance between a cylindrical plasma, an axial magnetic field and neutral gas, are explored further theoretically. The length of the cylinder is assumed much larger than its radius, so that axial losses are small and cross-field transport is dominant. Conditions for either magnetic pressure or neutrals pressure balancing the plasma pressure, and an associated coupling parameter, that were identified in the recent study are examined further. In addition, a second coupling parameter is identified that determines which is larger, the relative change in the magnetic field or the relative change in neutrals density. An unexpected nonmonotonic variation of the plasma density with the plasma particle flux is demonstrated. It is shown that for plasma beta close to unity, as plasma generation and plasma particle flux increase, the plasma density surprisingly decreases. The decrease follows a decrease of plasma confinement due to an increased plasma diamagnetism. The effect of the magnetic field on neutrals depletion is examined. It is shown that an increase of the magnetic field as the plasma density is kept constant, results in a decrease of neutrals depletion, while an increase of the magnetic field as the plasma particle flux is kept constant, results in constant neutrals depletion.

I. INTRODUCTION

Interesting nonlinear phenomena are observed in plasmas of high beta (the ratio of plasma pressure to magnetic pressure). Examples include, in laboratory plasmas, mirror and firehose instabilities [1], modified waves [2], and Alfven Ion Cyclotron (AIC) instabilities [3], and, in space, magnetic hole in a solar wind [4]. Diamagnetism is particularly a fundamental characteristic of high beta plasmas. A large diamagnetic current which modifies the magnetic field is expected to arise.

High temperature/energy plasmas in magnetic fusion devices and in certain plasma thrusters are candidates for reaching high beta. Such are the spherical tokamak, Field Reversed Configuration, and the MagnetoPlasmaDynamics thruster. However, often the magnetic pressure in high temperature plasmas is high so that the plasma beta turns out not to be high. Low temperature magnetized plasmas in which the magnetic field is low can be of a high beta, especially in plasma sources such as the helicon where the plasma density is relatively high [5]. Such low temperature plasmas are expected to be diamagnetic.

Diamagnetic currents and the associated magnetic field modification in low temperature plasmas have indeed been measured (for example, in [6–13]). Roberson et. al. [10] measured a large modification of the magnetic field in the plasma plume of a high power helicon. Takahashi and his colleagues described in several publications [11–13] measurements of the magnetic field modification in a helicon plasma thruster. From the modified magnetic field they evaluated the azimuthal diamagnetic current and calculated the thrust delivered by the magnetic pressure [11]. However, a few publications on high beta helicon plasma sources [6–9] reported magnetic reduction that was much smaller than expected by the plasma beta. Scime et. al. claimed that because their plasma is not in magnetohydrodynamic equilibrium, the magnetic field is only slightly reduced by the high-beta plasma [6]. Stenzel suggested that a radial electric field is excited that suppresses the diamagnetic current [7]. Corr and Boswell identified magnetic field penetration as the source of low diamagnetism [8]. It is important to explore further the causes of the often observed suppressed diamagnetism.

Suppression of diamagnetism in a low-temperature partially- ionized plasma was recently investigated experimentally [14] in the Large Helicon Plasma Device [15] and also in the Large Mirror Device [16]. The reduction of the magnetic field was measured as a function of the magnetic field for various argon gas pressures. The measurements were compared with

ing calculations by use of a theoretical model. It was demonstrated through the experiment and the theory that the suppression of the diamagnetic field can be caused by neutrals pressure. Neutrals depletion by the plasma pressure created a gradient of the neutrals pressure that partially balanced the gradient of the plasma pressure instead of the gradient of the magnetic field doing so, therefore the diamagnetism became weaker. Thus, in partially-ionized plasma there is a competition between the magnetic pressure and neutrals pressure in balancing the plasma pressure. This competition is reflected in the relative dominance of diamagnetism and neutrals depletion. The dominance in balancing the plasma pressure is not determined solely by the magnitudes of magnetic pressure and of neutrals pressure, but rather by the strength of the coupling of the plasma to the magnetic field relative to the strength of its coupling to the neutrals. The stronger the coupling is, the larger is the gradient, and accordingly, the larger is the change across the discharge, either of the magnetic pressure or of the neutrals pressure. In [14], a parameter was identified that determines which coupling is larger thus leading to the pressure change that is dominant.

Our purpose here is to explore further theoretically the competition between the magnetic pressure and neutrals pressure in balancing the plasma pressure. In Section II, we present the theoretical model for the plasma, the neutrals, and the magnetic field in a cylindrical configuration. The length of the cylindrical plasma discharge is assumed much larger than its radius, so that axial end losses are assumed small. The discharge described by a one-dimensional (1D) steady-state model, as radial dynamics is assumed dominant. Therefore, the model has to be modified in order to describe helicons in which axial dynamics is dominant. In Section III, two parameters that characterize the interaction, C_1 and C_2, are identified. They are called here coupling parameters although they vary radially across the discharge. The first coupling parameter, C_1, is reduced to the coupling parameter that was identified in [14], which determines which pressure change, that of the magnetic field or that of the neutrals, will balance the plasma pressure. The second coupling parameter, C_2, determines which is larger, the relative change in the magnetic field or the relative change in the neutrals density. Section IV presents an analytic solution of the linearized equations for low plasma density.

In Section V we calculate the plasma steady-state in two cases in which the neutrals pressure and the magnetic pressure are the same. However, the neutrals (gas) temperature and density are different in the two cases. As a result, the first of the two coupling parameters

has a different size in the two cases. The calculation shows that, although the pressures themselves are the same, in one case diamagnetism is dominant, while in the other case neutrals depletion is dominant.

In Section VI, the role of the second coupling parameter is demonstrated. It is shown how the relative changes of the magnetic field and of the neutrals density vary even if magnetic pressure and neutrals pressure are fixed. For different gases of identical such pressures, this second coupling parameter is different, resulting in different relative changes of the magnetic field and of the neutrals density. Also demonstrated here a somewhat unexpected effect. It is expected that as the rate of plasma generation increases, the plasma density should increase as well. It is shown that at a certain regime, an increase of the rate of generation results in a decrease of the plasma density, so that there is a nonmonotonic dependence of the plasma density on the rate of plasma generation.

In the last two sections, we examine the effect of the magnetic field on neutrals depletion, not necessarily related to diamagnetism. Neutrals depletion has been investigated theoretically extensively over the years (for example, [17–24]). It has been recently claimed [24] that neutrals depletion gets smaller when the magnetic field increases. It is shown in Section VII, that neutrals depletion indeed gets smaller with the magnetic field if the plasma density is kept constant. However, it is also shown that if the plasma radial particle flux is kept constant, then neutrals depletion is hardly affected by the variation of the magnetic field. Finally, conclusions are presented in Section VIII.

II. THE MODEL

We assume an azimuthally-symmetric partially-ionized cylindrical plasma that is immersed in a magnetic field parallel to the axis of symmetry denoted z axis, so that $\overrightarrow{B} = \widehat{e}_z B$. The length of the cylindrical plasma is assumed much larger than its radius, so that radial cross-field transport is dominant and axial transport along field lines is negligible. The short circuit effect of separate transport mechanisms for ions and electrons [23, 25] is also assumed negligible. The radial transport is ambipolar. As motion along magnetic field lines is neglected, the problem becomes one-dimensional where all variables depend on r only. The plasma and the neutral gas are assumed in steady-state, so that the equations are time-independent.

This manuscript was accepted by Phys. Plasmas. Click here to see the version of record.

Both plasma and neutrals are described by fluid equations. The plasma is described first. The momentum equations in the r, ϑ plane exhibit a force balance for the ions and for the electrons. In the radial direction there is balance between electric force, magnetic force, pressure gradient and collisions for the electrons:

$$-neE - \frac{\partial\left(nT_e\right)}{\partial r} - nev_{e\vartheta}B - nm_e\nu_{eN}\left(v_r - V_r\right) = 0, \tag{1}$$

and an equivalent force balance for the ions:

$$neE - \frac{\partial\left(nT_i\right)}{\partial r} + nev_{i\vartheta}B - nm_i\nu_{iN}\left(v_r - V_r\right) = 0. \tag{2}$$

In the azimuthal direction there is a balance between magnetic force and collisions for the electrons,

$$nev_rB - nm_e\nu_{ei}\left(v_{e\vartheta} - v_{i\vartheta}\right) - nm_e\nu_{eN}\left(v_{e\vartheta} - V_\vartheta\right) = 0, \tag{3}$$

and equivalently for the ions

$$-nev_rB - nm_i\nu_{ie}\left(v_{i\vartheta} - v_{e\vartheta}\right) - nm_i\nu_{iN}\left(v_{i\vartheta} - V_\vartheta\right) = 0. \tag{4}$$

Here, T_e and T_i are the electron and ion temperatures (in energy units), n is the density of the quasi-neutral plasma, e, m_i and m_e are the elementary charge and ion and electron masses, $v_{e\vartheta}$ and $v_{i\vartheta}$ are the electron and ion azimuthal velocities, v_r is the electron or the (equal) ion radial velocity, and V_r and V_ϑ are the components of the neutrals velocity. Also, ν_{ei} is electron-ion collision frequency, ν_{ie} the ion-electron, ν_{eN} the electron-neutral, and ν_{iN} the ion-neutral collision frequencies. In solving the equations, it is assumed here that there is no anomalous transport due to instabilities.

We note that as force balance was assumed, all inertia terms of the plasma have been omitted. The neglected inertia terms also included drag due to ionization and centripetal forces. We included all ion inertia terms in our previous publication [26]. In later publications [27–29], ion and electron inertia were included. Neither diamagnetism nor neutral depletion was addressed in these previous publications [26–29]. Inertia terms are important near the wall, where the ion velocity approaches the Bohm velocity, but these terms make little difference in the bulk of the plasma. It was shown in [27] that ignoring the electron inertia has a large effect on the solution near the wall, but has little effect on the solution of the problem as a whole. We assume that this holds for the ion inertia as well. Here, we neglect inertia terms and leave for future studies the inclusion in the model of those terms.

This manuscript was accepted by Phys. Plasmas. Click here to see the version of record.

We turn to the neutrals dynamics. In the radial direction there is a force balance between the neutrals pressure gradient and their collisions with the plasma,

$$\frac{\partial\left(NT_g\right)}{\partial r}-\left(nm_i\nu_{iN}+nm_e\nu_{eN}\right)\left(v_r-V_r\right)=0. \tag{5}$$

Here, n is the neutrals density and T_g their temperature. There should be a momentum equation for the neutrals in the azimuthal direction. In the azimuthal direction the drag by the plasma on the neutrals is balanced by neutral inertia terms. We skip writing the momentum equation for the neutrals in the azimuthal direction as the neutrals velocity in the azimuthal direction is assumed to be small.

The collision frequencies are now expressed as $\nu_{iN}=k_{iN}N$, $\nu_{eN}=k_{eN}N$, $\nu_{ei}=k_{ei}n$, and $\nu_{ie}=k_{ie}n$, where k_{iN}, k_{eN}, k_{ei}, and k_{ie} are collision rate constants. Since the net particle flux density is zero, the radial plasma particle flux density, $\Gamma=nv_r$, is related to the radial neutrals particle flux density, $\Gamma_N=NV_r$, as

$$\Gamma_N=-\Gamma. \tag{6}$$

The drag term in Eq. (5) can be expressed as $\left(m_ik_{iN}+m_ek_{eN}\right)\Gamma(N+n)$ and similarly the other drag terms. It is now assumed that $|V_r|$ is much smaller than v_r, or, equivalently, that N is much larger than n. These inequalities are not always strictly satisfied but for simplicity they are used through the numerical solutions here. The neutrals velocity components V_ϑ and V_r are thus neglected in the above equations.

By adding Eqs. (3) and (4), we obtain that $m_e\nu_{eN}v_{e\vartheta}+m_i\nu_{iN}v_{i\vartheta}=0$. Since $m_ek_{eN}\ll m_ik_{iN}$, it follows that $v_{i\vartheta}\ll v_{e\vartheta}$. We therefore neglect $v_{i\vartheta}$ relative to $v_{e\vartheta}$. We also neglect m_ek_{eN} relative to m_ik_{iN}.

We solve the above momentum equations for E, $v_{e\vartheta}$, and v_r and obtain the relations for the plasma particle flux density Γ

$$\Gamma=-\frac{\left(T_e+T_i\right)}{m_i\nu_i\left(\omega_c\omega_{ci}/\nu_i\nu_e+1\right)}\frac{\partial n}{\partial r}. \tag{7}$$

and for the ambipolar electric field

$$neE=\frac{\left[\left(\omega_c\omega_{ci}/\nu_i\nu_e\right)T_i-T_e\right]}{\left(\omega_c\omega_{ci}/\nu_i\nu_e+1\right)}\frac{\partial n}{\partial r}. \tag{8}$$

We assumed that T_e and T_i are uniform across the discharge. Here, $\omega_c\equiv eB/m_e$ and $\omega_{ci}\equiv eB/m_i$ are the electron and ion cyclotron frequencies, $\nu_e=k_{eN}N+k_{ei}n$, and $\nu_i=\nu_{iN}$.

This manuscript was accepted by Phys. Plasmas. Click here to see the version of record.

The electron-ion collision rate constant is taken as $k_{ei} = 2.9\times10^{-12}\ln\Lambda\, T_e^{-3/2}\,(\mathrm{eV})^{3/2}\ \mathrm{m^3\,s^{-1}}$, where $\ln\Lambda = 10$. The components of the electron velocity are $v_r = \Gamma/n$, where Γ is expressed through Eq. (7), and

$$v_{e\vartheta} = \left(\frac{\omega_c}{\nu_e}\right) v_r. \tag{9}$$

Note that the polarity of the electric field can reverse, even locally, depending on the sign of the numerator of Eq. (8). We assume here that $T_i \ll T_e$, and, moreover, that $(\omega_c\omega_{ci}/\nu_i\nu_e)\,T_i \ll T_e$, so that the electric field points radially outward, namely pushes the ions towards the wall, the same direction as without the magnetic field. However, the electric field is expected to be weaker when electrons are magnetized, as it is the magnetic field instead of the electric field that impedes their radial motion.

The momentum equations turn out therefore to be

$$T_e\frac{\partial n}{\partial r} = -m_i\nu_i\left(\frac{\omega_c\omega_{ci}}{\nu_i\nu_e}+1\right)\Gamma, \tag{10}$$

and

$$T_g\frac{\partial N}{\partial r} = m_i k_{iN} N\Gamma. \tag{11}$$

To the momentum equations, we add the continuity equation for the plasma,

$$\frac{1}{r}\frac{\partial\,(r\Gamma)}{\partial r} = \beta_{ion} N n. \tag{12}$$

The volume source term for the plasma is ionization, which is the sink term for the neutrals. The ionization rate coefficient is $\beta_{ion} = \sigma_0 v_{te}\exp\left(-\epsilon_i/T_e\right)$ [30], where $v_{te} \equiv (8T_e/\pi m_e)^{1/2}$ is the electron thermal velocity and $\sigma_0 \equiv \pi\left(e^2/4\pi\epsilon_0\epsilon_i\right)^2$, ϵ_0 being the vacuum permittivity and ϵ_i the ionization energy.

We turn now to the magnetic field. Employing Ampere's law, we write

$$\frac{\partial B}{\partial r} = \mu_0 e n v_{e,\vartheta}, \tag{13}$$

where μ_0 is the permeability of the vacuum. The contribution of the ions to the diamagnetic current has been neglected since the ion azimuthal velocity is much smaller than the electron azimuthal velocity, as explained above. Using Eq. (9), the gradient of the magnetic field is expressed as

$$\frac{\partial B}{\partial r} = \mu_0 e\frac{\omega_c}{\nu_e}\Gamma. \tag{14}$$

This manuscript was accepted by Phys. Plasmas. Click here to see the version of record.

Summing the four equations, while Eq. (14) is multiplied by B/μ_0, we obtain a total pressure balance:

$$nT_e + \frac{B^2}{2\mu_0} + NT_g = \frac{B_W^2}{2\mu_0} + N_W T_g. \tag{15}$$

Here, B_W and n_W are the magnetic field and neutrals density at the radial wall, where the plasma density is assumed to vanish, $n = 0$. Equation (15) can substitute one of the four other governing equations.

Equations (10), (11), (12) and (14) [or, equivalently, (15)] are the governing equations for Γ, n, N and B as functions of $r \in [0, a]$. Four boundary conditions are needed. Two of the boundary conditions are $\Gamma(0) = 0$ and $n(a) = 0$. For the neutrals density, either N_W or N_T, the total number of neutrals per unit length, $N_T = \int_0^a 2\pi r N dr$, is specified. For the magnetic field, either B_W, or the total magnetic flux, Φ_B, is specified. The total magnetic flux is $\Phi_B = \int_0^a 2\pi r B dr + B_W \pi \left(R^2 - a^2\right)$, where $R\,(\geq a)$ is the radius of the magnetic coil. In certain experiments it can be assumed that the magnetic flux does not change when the discharge is ignited, thus $\Phi_B = B_i \pi R^2$ where B_i is the magnetic field in the absence of the plasma. The temperatures T_e and T_g are determined by heat equations for the electrons and for the neutrals. Neutral-gas heating has been addressed (for example, [31, 32]). Here, T_g is specified. Also, since upon solving the equations we also specify either $n_0 \equiv n(0)$ or $\Gamma_W \equiv \Gamma(a)$, the electron temperature T_e becomes an eigenvalue that is determined through the solutions of the governing equations. In the solutions in this paper, N_W and B_W are specified (not N_T and Φ_B). Thus, the following relation is also available,

$$n_0 T_e + \frac{B_0^2}{2\mu_0} + N_0 T_g = \frac{B_W^2}{2\mu_0} + N_W T_g. \tag{16}$$

The magnetic field and the neutrals density on axis, $B_0 \equiv B\,(r = 0)$ and $N_0 \equiv N(r = 0)$ are found in the calculation, while n_0 is also specified (or found if, as stated above, Γ_W is specified).

III. DOMINANCE OF THE DIAMAGNETIC EFFECT

We identify here two parameters that determine the dominance of the diamagnetic effect. Equation (15) can be written as

$$P_n + P_B + P_N = P_{BW} + P_{NW}, \tag{17}$$

This manuscript was accepted by Phys. Plasmas. Click here to see the version of record.

where $P_n = nT_e$, $P_B = B^2/2\mu_0$ and $P_N = NT_g$ are the plasma, magnetic, and neutrals pressures, respectively, while $P_{BW} \equiv P_B(r=a) = B_W^2/2\mu_0$ and $P_{NW} = P_N(r=a) = N_W T_g$. We write equivalently the pressure balance as

$$\Delta P_n = \Delta P_B + \Delta P_N, \tag{18}$$

where $\Delta P_n \equiv n_0 T_e$ (the plasma pressure at the wall is assumed to vanish), $\Delta P_B \equiv \left(B_W^2 - B_0^2\right)/2\mu_0$, $\Delta P_N \equiv T_g \Delta N$, and $\Delta N \equiv N_W - N_0$. The change of the plasma pressure radially across the discharge is balanced by the sum of the change of the magnetic pressure due to the plasma diamagnetic current and of the change of the neutrals pressure due to neutrals depletion. The dominance of neutrals pressure in balancing the electron pressure was shown in [27] to lead to Boltzmann equilibrium. As demonstrated in [14], the diamagnetic effect is expressed by the first term in Eq. (10), while neutrals depletion is expressed by the second term in that equation. The change of the magnetic pressure is dominant when

$$\Delta P_B \geq \Delta P_N. \tag{19}$$

We emphasize that these are not the magnetic pressure or neutrals pressure themselves that determine which one of them will balance the plasma pressure, but rather these are the changes of these pressures across the discharge. The last equation can be written as

$$\frac{\Delta B}{B_W} \geq \frac{\Delta N}{N_W} \frac{\beta_N}{1 + B_0/B_W}. \tag{20}$$

Here $\Delta B \equiv B_W - B_0$ and the neutrals beta is defined here as

$$\beta_N \equiv \frac{2\mu_0 N_W T_g}{B_W^2}, \tag{21}$$

the ratio of the maximal neutrals pressure to maximal magnetic pressure. If inequality (19) is satisfied so that $\Delta P_B \gg \Delta P_N$, magnetic pressure only balances the plasma pressure, and

$$\frac{\Delta B}{B_W} \cong 1 - \sqrt{1 - \beta_n}. \tag{22}$$

The plasma beta is defined here as

$$\beta_n \equiv \frac{2\mu_0 n_0 T_e}{B_W^2}, \tag{23}$$

the ratio of the maximal plasma density to the maximal magnetic pressure.

This manuscript was accepted by Phys. Plasmas. Click here to see the version of record.

inequality (19) is satisfied, namely the magnetic pressure is dominant, if the first term on the right hand side (RHS) of Eq. (10) is larger than the second term. This happens if the parameter

$$C_1 \equiv \frac{\omega_c \omega_{ci}}{\nu_i \nu_e}. \tag{24}$$

is larger than unity, $C_1 > 1$. In that case, the contribution of the diamagnetic current to the pressure balance is dominant. When $C_1 < 1$, the change of neutrals pressure radially across the discharge is dominant. The changes (or gradients) of the pressures depend on the coupling of the plasma to the magnetic field through the diamagnetic current and to the neutrals through neutrals depletion. The parameter C_1 expresses the relative size of these couplings [14], the ratio of the coupling to the magnetic field over the coupling to the neutrals. We note that C_1 is not uniform across the discharge since it is a function of B, N, and n, which vary with r. Therefore inequality (24) may hold in part of the plasma only. The competition between the magnetic and neutrals pressure in balancing the plasma pressure is described through calculations in Sec. VI.

The electric field is also affected by C_1. From Eq. (8) it is seen that when T_i is negligible, the electric field in the bulk of the plasma is $E \approx T_e/(ea)$ for $C_1 \ll 1$, and is suppressed to $E \approx T_e/(eaC_1)$ for $C_1 \gg 1$.

It is interesting to compare the diamagnetism, the relative change of the magnetic field, to the neutrals depletion, the relative change of the neutrals density. This is important since if neutrals are depleted from the bulk of the discharge, the discharge may not be sustained. In particular, we would like to find out when

$$\frac{\Delta B}{B_W} \geq \frac{\Delta N}{N_W}. \tag{25}$$

We note that the magnetic pressure can be dominant, so that inequality (19) [or in its form (20)] is satisfied, but, as $\beta_N/(1 + B_0/B_W)$ is smaller than unity, inequality (25) is not satisfied and neutrals are completely depleted. In order to examine the relation between the relative changes [Eq. (25)], We note that Eqs. (11) and (14) can be written as

$$\frac{\partial \ln N}{\partial r} = \frac{m_i k_{iN}}{T_g}\Gamma, \qquad \frac{\partial \ln B}{\partial r} = \frac{\mu_0 e^2}{m_e \nu_e}\Gamma. \tag{26}$$

In order for inequality (25) to be satisfied, the parameter

$$C_2 \equiv \frac{\mu_0 e^2 T_g}{m_e \nu_e m_i k_{iN}} \tag{27}$$

This manuscript was accepted by Phys. Plasmas. Click here to see the version of record.

ing to be larger than unity. Note that

$$C_2 = C_1 \frac{\beta_N}{2} \frac{B_W^2}{B^2}. \tag{28}$$

The effect of varying C_2 will be discussed in Sec. VII.

IV. LINEAR ANALYSIS

Before presenting a full numerical solution of the governing equations, we present a simplified linear analysis (which was first presented in [14]).

We assume that the plasma pressure is small, so that neutrals depletion and the diamagnetic effect are small, and the variations of the magnetic field and of the neutrals density are small. We solve the equations iteratively. To zeroth order, we assume that the magnetic field and the neutrals density are constant. The equations are not linear since the electron collision frequency ν_e depends on the plasma density that varies radially. We nevertheless substitute $n(r) = n_0$ in the expression for ν_e, so that it is constant as well across the discharge. The equations in zeroth order are thus linear with constant coefficients. Equations (12) and (10) are combined in a standard way to $(1/r)\,\partial/\partial r\,(r\partial n/\partial r) = -\left[\alpha\,(C_1+1)\,/a^2\right] n$, where $\alpha \equiv \beta_{ion} m_i \nu_i N_W a^2/T_e$ and

$$C_1 = \frac{e^2 B_W^2}{m_e m_i \nu_i \nu_e}. \tag{29}$$

The coefficients α and C_1 are taken as constant and for ν_e the electron density is taken as n_0. Using the boundary condition $n(a) = 0$, we write the plasma density and particle flux density as

$$n = n_0 J_0\left(\frac{p_1 r}{a}\right), \quad \Gamma = \left[\frac{n_0 T_e}{m_i \nu_i a\,(C_1+1)}\right] p_1 J_1\left(\frac{p_1 r}{a}\right). \tag{30}$$

Here, J_0 and J_1 are the Bessel functions of zeroth and first order, and $p_1 = 2.4048$ is the first zero of J_0. The resulting solvability condition, $\sqrt{\alpha\,(C_1+1)} = p_1$, determines the value of the eigenvalue T_e. It was shown in [23], that if ν_e varies with n, the density profile is more convex than the Bessel function $J_0\,(p_1 r/a)$ is.

The perturbed first-order neutrals density and magnetic field are obtained using the zeroth order expressions for n and for Γ. The neutrals density is approximately

$$N = N_W - \left[\frac{1}{(C_1+1)} \frac{n_0 T_e}{T_g}\right] J_0\left(\frac{p_1 r}{a}\right). \tag{31}$$

The magnetic field is approximately

$$B = B_W - \left[\frac{C_1}{(C_1+1)}\frac{\mu_0 n_0 T_e}{B_W}\right] J_0\left(\frac{p_1 r}{a}\right). \tag{32}$$

We therefore write

$$\frac{\Delta N}{N_W} = \frac{1}{(C_1+1)}\frac{n_0 T_e}{N_W T_g}; \qquad \frac{\Delta B}{B_W} = \frac{C_1}{(C_1+1)}\frac{\beta_n}{2}. \tag{33}$$

Substituting these expressions into Eq. (20), with $1+B_0/B_W \cong 2$, we find that, as expected, inequalities (19) and (20) hold when $C_1 \geq 1$. Also according to (33), the relative change in B is larger than the relative change in N if

$$C_1\frac{\beta_N}{2} \geq 1. \tag{34}$$

It is easy to verify that $C_2 = C_1\beta_N/2$, so the condition is

$$C_2 = C_1\frac{\beta_N}{2} \geq 1, \tag{35}$$

as expected.

When $C_1 \gg 1$, the diamagnetic effect is noticeable, $\Delta B/B_W \cong \beta_n/2$, while $\Delta N/N_W \ll n_0 T_e/N_W T_g$, and when $C_1 \ll 1$, the diamagnetic effect is small, $\Delta B/B_W \ll \beta_n/2$, while the change in the neutrals pressure across the discharge due to neutrals depletion is large and balances the plasma pressure, $\Delta N/N_W \cong n_0 T_e/N_W T_g$.

V. DIAMAGNETISM VERSUS NEUTRALS DEPLETION

In this section we present two cases, case A and case B. The magnetic pressure is the same in the two plasma steady-states of the two cases and so is the neutrals pressure. However, the neutrals temperature in case A is lower than it is in case B, and correspondingly, since the neutrals pressure is the same, the neutrals density is higher in case A. As a result of the higher neutrals density, ion-neutrals collisions are more frequent in case A. This is expressed in a lower C_1 in case A. The calculation shows that, as expected, neutrals depletion is more pronounced in case A than in case B, while diamagnetism is more pronounced in case B.

Let us describe the plasma in cases A and B. An argon plasma in a cylindrical tube of radius $a = 0.1\,\mathrm{m}$ is confined by a magnetic field of $B_W = 50\,\mathrm{G}$, so that $P_B(r=a) = 9.95\,\mathrm{Pa}$, while the gas pressure at the wall is $P_N(r=a) = N_W T_g = 4\,\mathrm{Pa}$. Therefore, $\beta_N \cong 0.4$.

This manuscript was accepted by Phys. Plasmas. Click here to see the version of record.

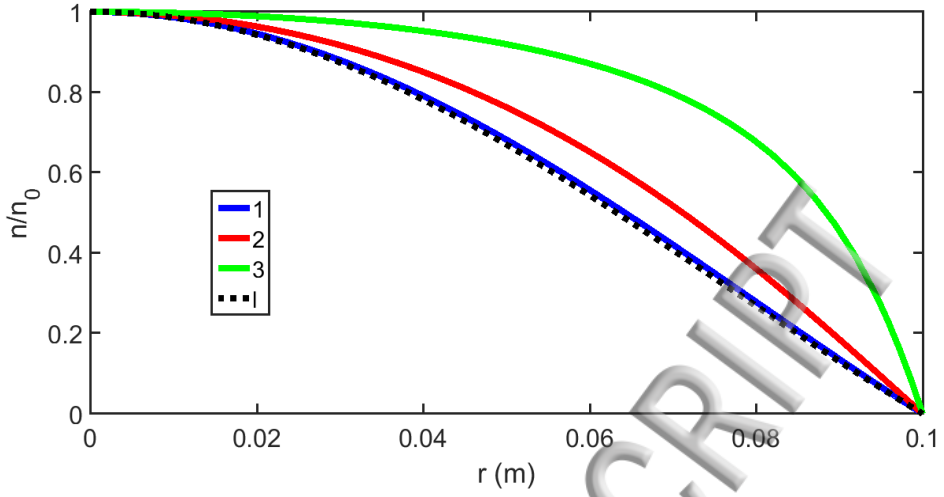

FIG. 1: Case A (argon, $T_g = 300\,\mathrm{K}, P_{NW} = 4\,\mathrm{Pa}, B_W = 50\,\mathrm{G}, a = 0.1\,\mathrm{m}$). Normalized plasma density profiles n/n_0 for three plasma densities, 1) $n_0 = 10^{18}\,\mathrm{m}^{-3}$, 2) $n_0 = 6.5 \times 10^{18}\,\mathrm{m}^{-3}$, and 3) $n_0 = 1.3 \times 10^{19}\,\mathrm{m}^{-3}$. For the lowest density, denoted as 1 (blue - online), the profile coincides with the linear solution (dashed line) [Eq. (30)]. As the plasma density is higher, the profile is more convex.

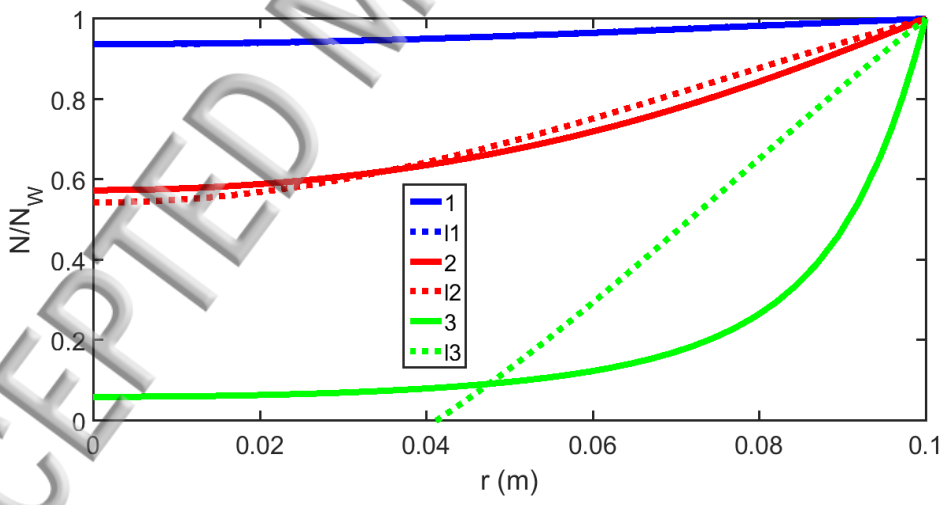

FIG. 2: Case A (argon, $T_g = 300\,\mathrm{K}, P_{NW} = 4\,\mathrm{Pa}, B_W = 50\,\mathrm{G}, a = 0.1\,\mathrm{m}$). Normalized neutrals density profiles (N/N_W) due to neutrals depletion for the three plasma densities as in Fig. 1. The dotted lines show the approximated expression, Eq. (31), where l1, l2 and l3 denote neutrals density profiles for the three plasma densities in an increasing order. The higher n_0 is, the lower is the neutrals density.

For argon, $\epsilon_i = 15.6\,\mathrm{eV}$ and $k_{eN} = 1.3 \times 10^{-13}\,\mathrm{m^3\,s^{-1}}$ [30]. We also use in the calculation for argon $k_{iN} = 6.3 \times 10^{-16}\,\mathrm{m^3/\,s}$ [30], although in order to reach an agreement with the experiment, we sometimes used in our previous publication [14] a larger value for k_{iN} .

Case A is discussed first. In case A, presented in Figs. 1 - 4, the gas temperature is $T_g = 300\,\mathrm{K}$ and the full equations are solved for three plasma densities, $n_0 = 10^{18}\,\mathrm{m^{-3}}$, $n_0 = 6.5 \times 10^{18}\,\mathrm{m^{-3}}$, and $n_0 = 1.3 \times 10^{19}\,\mathrm{m^{-3}}$. It is found that T_e increases with n_0, and T_e is 1.8 eV, 1.9 eV, and 2.7 eV for the three plasma densities. Figure 1 shows the radial profiles of the normalized plasma density for the three plasma densities. For a higher plasma density, the plasma profile is more convex. The dashed line denotes the radial profile of the linear solution [Eq. (30)]. Figure 2 shows the radial profiles of the normalized neutrals density for the three plasma densities. As expected, for a higher plasma density, neutrals depletion is larger. Figure 3 shows the radial profiles of the magnetic field for the three plasma densities. As expected also here, for a higher plasma density, the diamagnetic effect is larger. The neutrals density and the magnetic field obtained by solving the linearized equations are also shown for the three densities in Figures 2 and 3. It is seen in these figures (and in Fig. 1), that Eqs. (30), (31), and (32) are a good approximation for the profiles of n, N and B for the lowest plasma density but are not such a good approximation for the two higher plasma densities.

In Figures 2 and 3, it is seen that $\Delta B/B_W \ll \Delta N/N_W$. For example, for the case of the highest plasma density of the three cases shown, $\Delta B/B_W \cong 0.1$, while $\Delta N/N \cong 0.95$. This larger neutrals depletion is in agreement with Eqs. (25) and (27), as C_2 is much smaller than unity. Let us show that C_2 is smaller than unity. Since $\beta_N \cong 0.4$, and since $B/B_W \approx 1$ for the three densities, it follows from Eq. (35) that $C_2 \simeq 0.2C_1$. The values of C_1, defined for $B = B_W$, $n = n_0$ and $N = N_W$, for the three different plasma densities are 0.13, 0.09,and 0.08, so that indeed $C_2 \ll 1$. The relative change in the magnetic field, $\Delta B/B_W \cong 0.1$, is considerably smaller than the value predicted by Eq. (22), which is $1 - \sqrt{1-\beta_n} = 0.19$ (here, $\beta_n = 0.57$).

We now examine the competition between magnetic pressure and neutrals pressure in balancing the plasma pressure in case A. As described above, $C_1 < 1$ for all three plasma densities of case A, and, therefore, following Eqs. (19) - (24), the plasma pressure gradient is mostly balanced by the neutrals pressure gradient; neutrals depletion is dominant. Figure 4 shows the profiles of the various pressures for the highest plasma density, $n_0 = 1.3 \times 10^{19}\,\mathrm{m^{-3}}$.

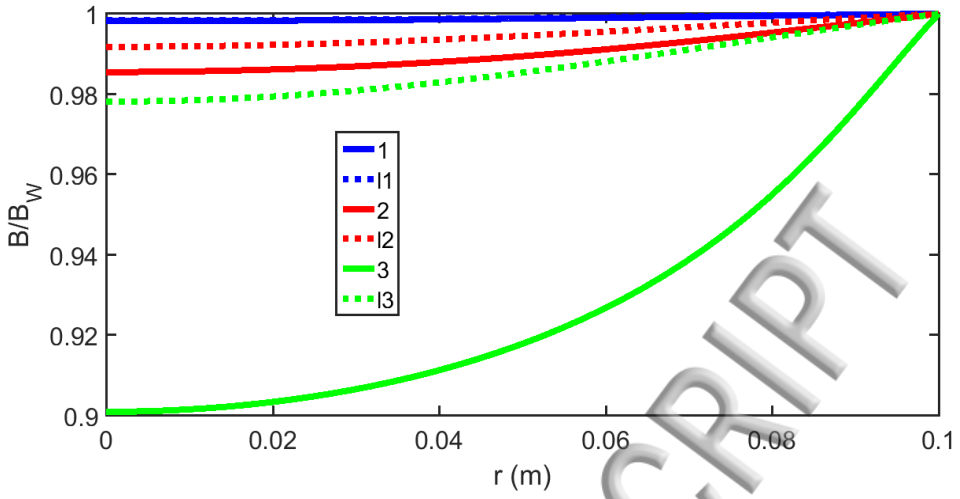

FIG. 3: Case A (argon, $T_g = 300\,\mathrm{K}, P_{NW} = 4\,\mathrm{Pa}, B_W = 50\,\mathrm{G}, a = 0.1\,\mathrm{m}$). Normalized magnetic field profiles (B/B_W) due to diamagnetic currents for the three plasma densities as in Fig. 1. The dotted lines show the approximated expression, Eq. (32), where l1, l2 and l3 denote magnetic field profiles for the three plasma densities in an increasing order. The higher n_0 is, the lower is the magnetic field.

It is seen that $\Delta P_B < 2\,\mathrm{Pa}$ while $\Delta P_N \cong 4\,\mathrm{Pa}$.

In case B, shown in Figs. 5 - 7, the gas pressure is $P_N\,(r = a) = N_W T_g = 4\,\mathrm{Pa}$, the same as in case A shown in Figs. 1 - 4. However, the gas temperature is $T_g = 1800\,\mathrm{K}$, 6 times higher than in the case A, so that the neutrals density is 6 times smaller. Characteristic values of C_1 are 3.7, 1.4,and 1.1 for the three different plasma densities, $n_0 = 10^{18}\,\mathrm{m}^{-3}$, $n_0 = 8 \times 10^{18}\,\mathrm{m}^{-3}$ and $n_0 = 1.6 \times 10^{19}\,\mathrm{m}^{-3}$. The electron temperature T_e increases with n_0, and T_e is 2.4 eV, 2.7 eV, and 3.3 eV for the three plasma densities, higher than in the previous case. Figures 5 and 6 show the radial profiles of the normalized neutrals density and magnetic field intensity for the three plasma densities in case B (equivalently to Figures 2 and 3 of case A). Also shown in the figures are those radial profiles as found from the linear approximations, which are a good approximation for the lower plasma densities. As expected, and similarly to Figures 2 and 3 of case A, Neutrals depletion and diamagnetism are larger for a higher plasma density. As is seen in Figures 5 and 6, in case B, $\Delta B/B_W$ is smaller than $\Delta N/N_W$ as well. However, $(\Delta B/B_W)\,/\,(\Delta N/N_W)$ in case B is not as small as it is in case A. Moreover, as $C_1 > 1$ in case B, the plasma pressure is mostly balanced by the magnetic pressure. This is demonstrated in Fig. 7, where $\Delta P_B \cong 6\,\mathrm{Pa}$, while $\Delta P_N < 3\,\mathrm{Pa}$.

This manuscript was accepted by Phys. Plasmas. Click here to see the version of record.

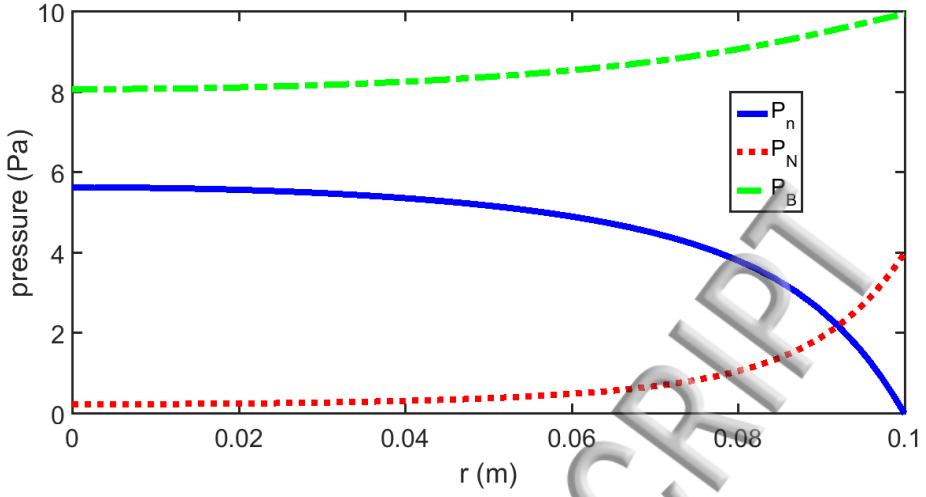

FIG. 4: Case A (argon, $T_g = 300\,\mathrm{K}, P_{NW} = 4\,\mathrm{Pa}, B_W = 50\,\mathrm{G}, a = 0.1\,\mathrm{m}$). Magnetic pressure P_B, Neutrals pressure P_N and plasma pressure P_n for $n_0 = 1.3 \times 10^{19}\,\mathrm{m}^{-3}$. Neutrals pressure is dominant over magnetic pressure: $\Delta P_N > \Delta P_B$.

Figures 1 - 7, and especially Figs. 4 and 7, in which cases A and B are compared, demonstrate that it is the coupling between the plasma and the neutrals that determines the role of neutrals in suppression of diamagnetism, rather than the sizes of the magnetic pressure and neutrals pressure themselves. Although the magnetic pressure and the neutrals pressure are the same in both cases, in case A, neutral pressure is dominant, while in case B, magnetic pressure is dominant.

VI. NONMONOTONIC DENSITY DEPENDENCE

In this section, a nonmonotonic dependence of the plasma density n_0 on the particle flux $\Gamma_W = \Gamma(r = a)$ is demonstrated. A physical explanation is provided to this somewhat unexpected behavior. In addition, we examine what is larger, the relative change of neutrals density $\Delta N/N_W$ or the relative change in the magnetic field $\Delta B/B_W$. As mentioned above, the parameter C_2 [defined in Eq. (27)] determines which of the two is dominant. For a larger C_2, $(\Delta B/B_W)\,/\,(\Delta N/N_W)$ is expected to be larger. The parameter C_2 is larger when the gas temperature is higher or when the ion mass is smaller. We calculate the steady states for three different discharges, for which C_2 is different. Case C is of argon discharge with gas at room temperature. Case D is of the lighter helium at room temperature, and case E

This manuscript was accepted by Phys. Plasmas. Click here to see the version of record.

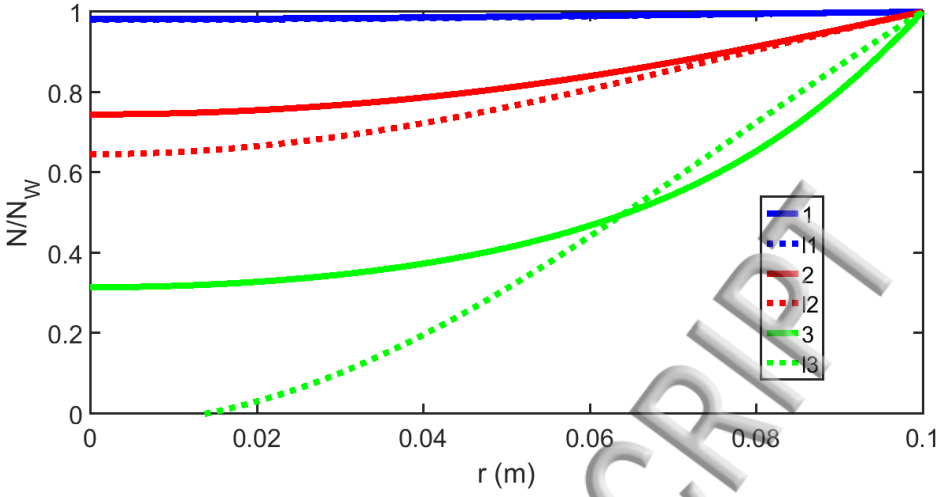

FIG. 5: Case B (argon, $T_g = 1800\,\mathrm{K}, P_{NW} = 4\,\mathrm{Pa}, B_W = 50\,\mathrm{G}, a = 0.1\,\mathrm{m}$). Normalized neutrals density profiles (N/N_W) due to neutrals depletion for three plasma densities, 1) $n_0 = 10^{18}\,\mathrm{m}^{-3}$, 2) $n_0 = 8 \times 10^{18}\,\mathrm{m}^{-3}$, and 3) $n_0 = 1.6 \times 10^{19}\,\mathrm{m}^{-3}$. As in Fig. 2, the dotted lines show the approximated expression, Eq. (31), where l1, l2 and l3 denote neutrals density profiles for the three plasma densities in an increasing order. The higher n_0 is, the lower is the neutrals density.

is of helium of a higher gas temperature. It is shown that indeed $(\Delta B/B_W)\,/\,(\Delta N/N_W)$ is largest in case E and smallest in case C.

In all three cases, C, D and E, the discharge is in a cylindrical tube of radius $a = 0.1\,\mathrm{m}$, and the plasma is confined by an axial magnetic field, as in the cases A and B. In cases C, D and E, however, the magnetic field is $B_W = 150\,\mathrm{G}$, higher than in cases A and B, so that the magnetic pressure here is $P_{BW} = 90\,\mathrm{Pa}$. The gas pressure is $P_{NW} = N_W T_g = 0.5\,\mathrm{Pa}$, lower than in cases A and B. Therefore, $P_B \gg P_N$ and $\beta_N = 0.0056$. Moreover, for these parameter values in cases C, D, and E, it turns out that $C_1 \gg 1$, so that the plasma pressure is expected to be balanced mostly by the gradient of the magnetic pressure. Therefore, it follows that in cases C, D, and E presented in Figs. 8 - 14, $\Delta B/B_W \cong 1 - \sqrt{1-\beta_n}$ (this relation is not shown in the figures). Although $C_1 \gg 1$, it is not clear whether C_2 is large as well. Indeed, C_2 is different for cases C, D, and E, and, as a result, $(\Delta B/B_W)\,/\,(\Delta N/N_W)$ is also different in the three cases.

We start with case C, an argon discharge with $T_g = 300\,\mathrm{K}$. Figures 8 - 10 describe the calculations for case C. The above-mentioned unexpected nonmonotonic variation of the plasma density with the plasma particle flux density is seen in Fig. 8. We note that Γ_W, the

This manuscript was accepted by Phys. Plasmas. Click here to see the version of record.

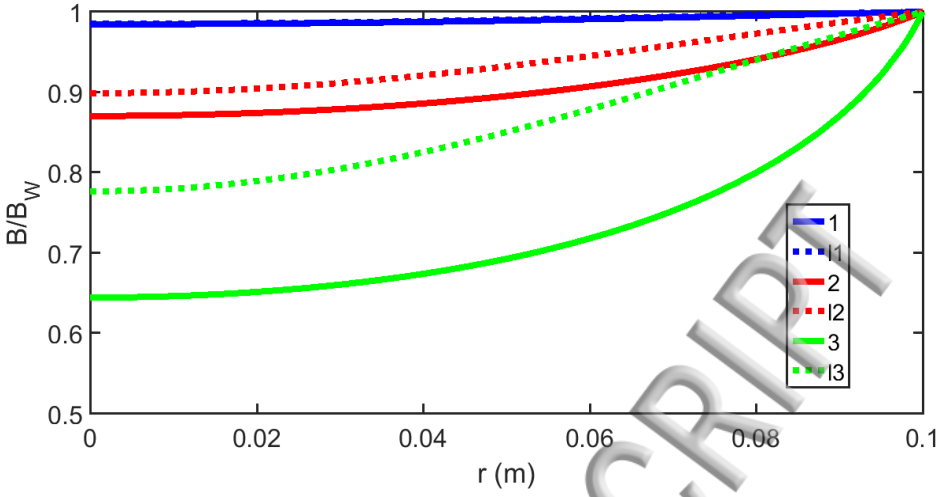

FIG. 6: Case B (argon, $T_g = 1800\,\mathrm{K}, P_{NW} = 4\,\mathrm{Pa}, B_W = 50\,\mathrm{G}, a = 0.1\,\mathrm{m}$). Normalized magnetic field profiles (B/B_W) due to diamagnetic currents for the three argon plasma densities and the same parameters as in Fig. 5. As in Fig. 3, the dotted lines show the approximated expression, Eq. (32), where l1, l2 and l3 denote magnetic field profiles for the three plasma densities in an increasing order. The higher n_0 is, the lower is the magnetic field.

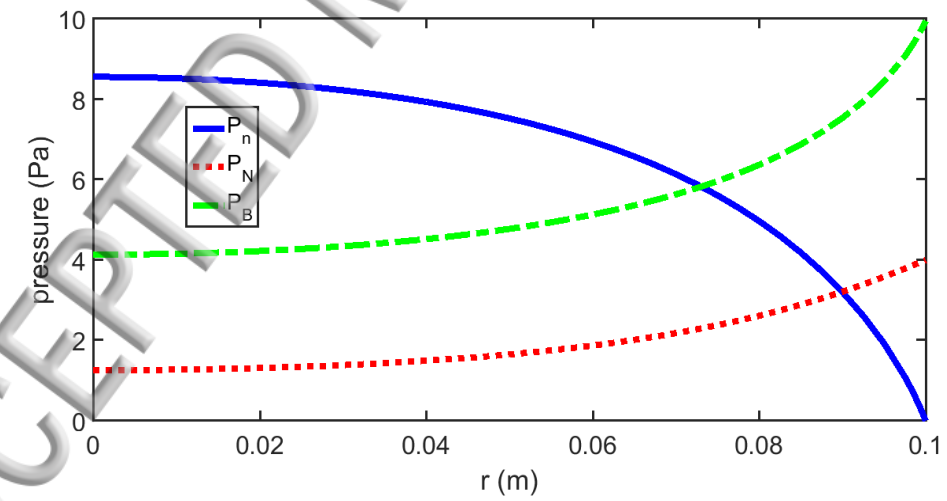

FIG. 7: Case B (argon, $T_g = 1800\,\mathrm{K}, P_{NW} = 4\,\mathrm{Pa}, B_W = 50\,\mathrm{G}, a = 0.1\,\mathrm{m}$). Magnetic pressure P_B, Neutrals pressure P_N and plasma pressure P_n for $n_0 = 1.6 \times 10^{19}\,\mathrm{m}^{-3}$. The same magnetic pressure and neutrals pressure at the wall as in Fig. 4, but magnetic pressure is dominant here over neutrals pressure, $\Delta P_B > \Delta P_N$.

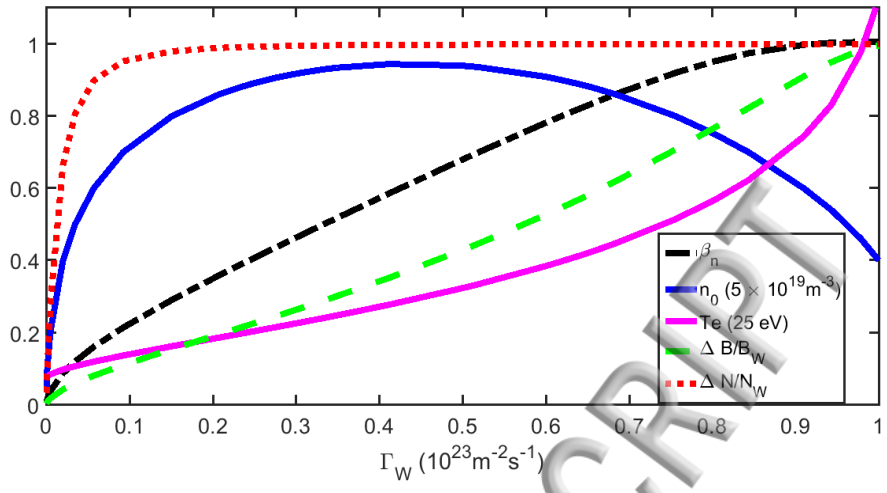

FIG. 8: Case C (argon, $T_g = 300\,\mathrm{K}$, $P_{NW} = 0.5\,\mathrm{Pa}$, $B_W = 150\,\mathrm{G}$, $a = 0.1\,\mathrm{m}$). Electron temperature T_e (solid, magenta), plasma density n_0 (solid, nonmonotonic, blue), plasma beta β_n (dashed - dotted, black), $\Delta B/B_W$ (dashed, green) and $\Delta N/N_W$ (dotted, red) versus plasma flux density Γ_W. Nonmonotonic variation of n_0 due to the increase of cross-field transport with Γ_W; $\Delta N/N_W \gg \Delta B/B_W$.

plasma particle flux density, also represents the rate of plasma generation through Eq. (12). At lower values of Γ_W, an increase of Γ_W results in an increase of n_0, the plasma density, as expected. However, for higher Γ_W, the plasma density decreases with the increase of Γ_W. This unexpected nonmonotonic dependence of the plasma density on the plasma particle flux density is a result of a varying cross-field transport. The plasma density is determined by both the generation rate (expressed in the flux density Γ_W) and by the residence time of the plasma in the dischrge volume. The residence time is shorter as cross-field transport is faster. At low values of Γ_W and when the diamagnetic effect is small, an increase of the generation rate of the plasma (and of Γ_W) results in a higher plasma density. However, when the plasma generation rate is high, the significant diamagnetic effect results in a lower magnetic field and a faster cross-field transport. The residence time of the plasma becomes shorter. As a result, the plasma density decreases. It is somewhat counter-intuitive behavior - although more plasma is generated, the plasma density is lower.

A nonmonotonic dependence of the plasma density on the plasma particle flux was also found in an unmagnetized plasma [22]. The reason for the nonmonotonic dependence was similar. The plasma residence time was shorter and the transport faster for a high plasma

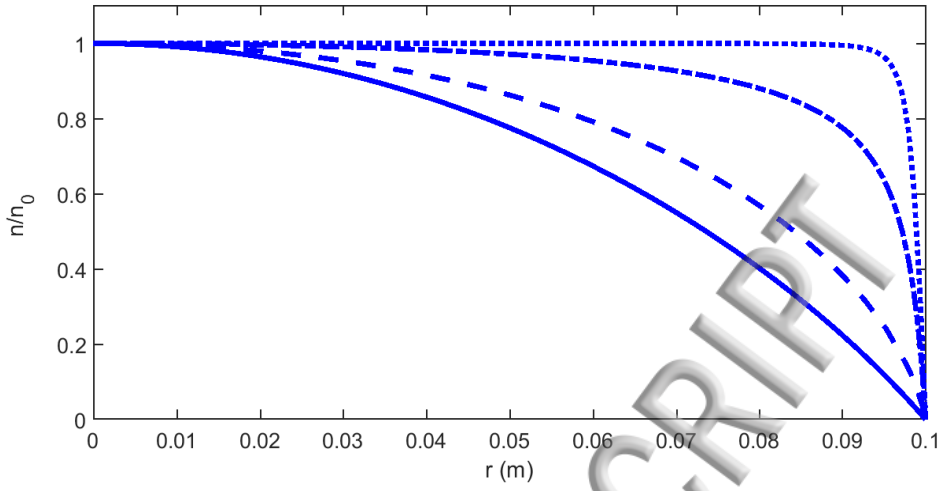

FIG. 9: Case C (argon, $T_g = 300\,\mathrm{K}$, $P_{NW} = 0.5\,\mathrm{Pa}$, $B_W = 150\,\mathrm{G}, a = 0.1\,\mathrm{m}$). Radial profiles of plasma density n/n_0 for various plasma particle flux densities Γ_W. The most concave profile is at the linear limit: 1) $\Gamma_W = 5\times10^{19}\,\mathrm{m^{-2}\,s^{-1}}$ ($n_0 = 2.5\times10^{18}\,\mathrm{m^{-3}}$, $T_e = 1.9\,\mathrm{eV}$, negligible diamagnetism and neutrals depletion) - solid. The other three profiles are for : 2) $\Gamma_W = 2\times10^{21}\,\mathrm{m^{-2}\,s^{-1}}$ ($n_0 = 2\times10^{19}\,\mathrm{m^{-3}}$, $T_e = 2.5\,\mathrm{eV}$) - dashed, 3) $\Gamma_W = 6\times10^{22}\,\mathrm{m^{-2}\,s^{-1}}$ ($n_0 = 4.55\times10^{19}\,\mathrm{m^{-3}}$, $T_e = 9.6\,\mathrm{eV}$) - dashed-dotted, and 4) $\Gamma_W = 1\times10^{23}\,\mathrm{m^{-2}\,s^{-1}}$ ($n_0 = 2\times10^{19}\,\mathrm{m^{-3}}$, $T_e = 28\,\mathrm{eV}$) - dotted. As Γ_W is larger, the plasma density profile is more convex.

particle flux. Neutrals depletion decreased the number of neutrals and weakened the drag on the ions. In that previous case [22], it was neutrals depletion that allowed faster plasma transport to the wall, while in our case here, it is plasma diamagnetism that allows such a fast transport.

As is seen in Fig. 8, the plasma beta, β_n, increases with Γ_W. As Γ_W increases, the plasma density n_0 decreases and the temperature T_e increases, so that β_n, which is proportional to n_0T_e, gets closer to unity.

As Γ_W increases, both diamagnetism and neutrals depletion increase; $\Delta B/B_W$ and $\Delta N/N_W$ increase and eventually reach unity. However, neutrals depletion is dominant, $\Delta N/N_W$ is much larger than $\Delta B/B_W$. Neutrals density, $\Delta N/N_W$, gets closer to unity at much smaller Γ_W than diamagnetism, $\Delta B/B_W$, does. As is seen in Fig. 8, $\Delta N/N_W$ is nearly unity already for $\Gamma_W = 5\times10^{21}\,\mathrm{m^{-2}\,s^{-1}}$, while $\Delta B/B_W \simeq 0.02$ at that flux density, and becomes nearly unity for $\Gamma_W \cong 10^{23}\,\mathrm{m^{-2}\,s^{-1}}$ only. This larger neutrals depletion is a result of C_2 being smaller than unity everywhere except very close to the wall. This relation

This manuscript was accepted by Phys. Plasmas. Click here to see the version of record.

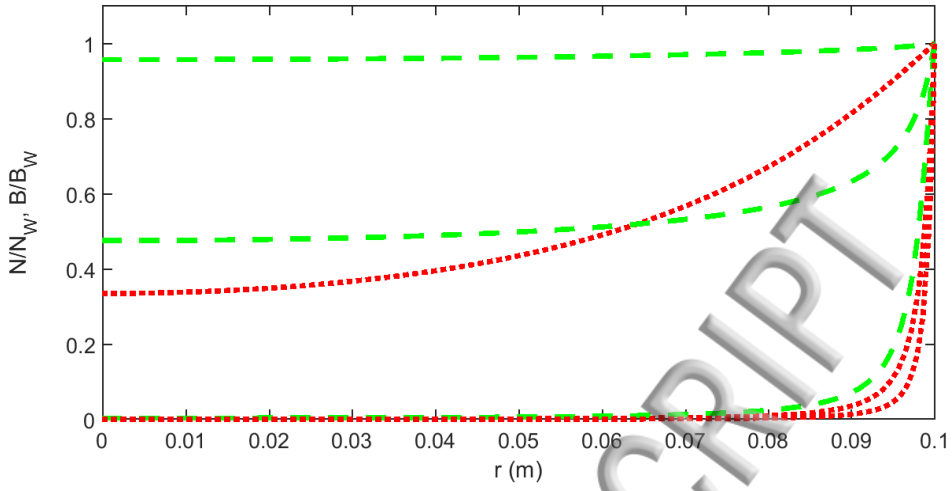

FIG. 10: Case C (argon, $T_g = 300\,\mathrm{K}$, $P_{NW} = 0.5\,\mathrm{Pa}$, $B_W = 150\,\mathrm{G}, a = 0.1\,\mathrm{m}$). Radial profiles of $\Delta N/N_W$ (dotted, red) and of $\Delta B/B_W$ (dashed, green) for 1) $\Gamma_W = 2\times10^{21}\,\mathrm{m^{-2}\,s^{-1}}$ ($n_0 = 2\times10^{19}\,\mathrm{m^{-3}}$, $T_e = 2.5\,\mathrm{eV}$), 2) $6\times10^{22}\,\mathrm{m^{-2}\,s^{-1}}$ ($n_0 = 4.55\times10^{19}\,\mathrm{m^{-3}}$, $T_e = 9.6\,\mathrm{eV}$), and 3) $1\times10^{23}\,\mathrm{m^{-2}\,s^{-1}}$ ($n_0 = 2\times10^{19}\,\mathrm{m^{-3}}$, $T_e = 28\,\mathrm{eV}$). As Γ_W is larger, $\Delta N/N_W$ and $\Delta B/B_W$ are larger. $\Delta N/N_W \gg \Delta B/B_W$, except for the highest Γ_W when both $\Delta N/N_W$ and $\Delta B/B_W$ are close to unity. Neutrals depletion is much more pronounced than the diamagnetic effect.

between neutrals depletion and diamagnetism in case C can be explained. Often, and also here, $k_{ei}n_0 > k_{eN}N_W$, so that $\nu_e \cong k_{ei}n_0$. From Eq. (27), it can be seen that in such a case, for C_2 to be larger than unity, so that $\Delta B/B_W > \Delta N/N_W$, the plasma density has to satisfy $n_0 < \mu_0 e^2 T_g/\left(m_e k_{ei} m_i k_{iN}\right)$. In case C, of argon with gas at room temperature, the inequality is reduced to $n_0 < 1.2\times10^{17}\,\mathrm{m^{-3}}\;T_e^{3/2}\,(\mathrm{eV})^{-3/2}$. Taking into account electron-neutral collisions would mean that the plasma density has to be even smaller. For $B_W = 150\,\mathrm{G}$ and T_e of few eV, the requirement on the plasma density means that β_n has to be much smaller than unity so that $\Delta B/B_W$ be comparable to $\Delta N/N_W$. However, a necessary condition for $\Delta B/B_W$ to be noticeable is that β_n is on the order of unity. Therefore, for the parameters of case C, when $\Delta B/B_W$ is noticeable, $C_2 < 1$, and $\Delta B/B_W$ is smaller than $\Delta N/N_W$, as demonstrated in Fig. 8.

The radial profiles of the normalized plasma density n/n_0 are shown in Fig. 9, and normalized neutrals density N/N_W and magnetic field B/B_W are shown in Fig. 10, all in case C, for three plasma particle flux densities, $\Gamma_W = 2\times10^{21}\,\mathrm{m^{-2}\,s^{-1}}$, $6\times10^{22}\,\mathrm{m^{-2}\,s^{-1}}$, and $1\times10^{23}\,\mathrm{m^{-2}\,s^{-1}}$. The plasma densities that correspond to the three flux densities are

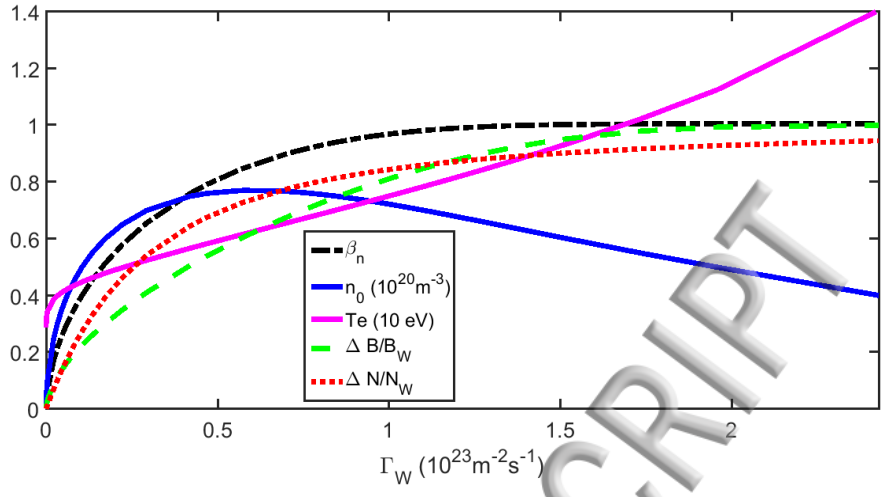

FIG. 11: Case D (helium, $T_g = 300\,\mathrm{K}$, $P_{NW} = 0.5\,\mathrm{Pa}$, $B_W = 150\,\mathrm{G}$, $a = 0.1\,\mathrm{m}$). Electron temperature T_e (solid, magenta), plasma density n_0 (solid, nonmonotonic, blue), plasma beta β_n (dashed - dotted, black), $\Delta B/B_W$ (dashed, green) and $\Delta N/N_W$ (dotted, red) versus plasma flux density Γ_W. Nonmonotonic variation of n_0 due to the increase of cross-field transport with Γ_W; $\Delta N/N_W$ and $\Delta B/B_W$ are similar in magnitude.

$n_0 = 2 \times 10^{19}\,\mathrm{m}^{-3}$, $4.5 \times 10^{19}\,\mathrm{m}^{-3}$, and again $2 \times 10^{19}\,\mathrm{m}^{-3}$, respectively. The electron temperatures are $T_e = 2.5\,\mathrm{eV}$, $9.6\,\mathrm{eV}$ and $28\,\mathrm{eV}$, respectively. Also shown in Fig. 9 is the plasma density profile (the most concave) for $\Gamma_W (= 5 \times 10^{19}\,\mathrm{m}^{-2}\,\mathrm{s}^{-1})$ that is so low that diamagnetism and neutrals depletion are negligible. For this low Γ_W, the maximal plasma density is $n_0 = 2.5 \times 10^{18}\,\mathrm{m}^{-3}$ and $T_e = 1.9\,\mathrm{eV}$. For this low Γ_W, the neutrals density and magnetic field are uniform and thus are not shown in Fig 10. As Γ_W is higher, the plasma density profile in Fig. 9 is more convex and the neutrals density and magnetic field are lower. As was also clear from Fig. 8, neutrals depletion is much more pronounced than the diamagnetic effect, $\Delta N/N_W \gg \Delta B/B_W$, except for the highest Γ_W when both $\Delta N/N_W$ and $\Delta B/B_W$ are close to unity. Note that, because of the nonmonotonic dependence of the plasma density, the first curve (second for n/n_0) and the third curve (fourth for n/n_0) are for the same plasma density, $n_0 = 2 \times 10^{19}\,\mathrm{m}^{-3}$. However, the first curve corresponds to low temperature, $T_e = 2.5\,\mathrm{eV}$, low beta, and low diamagnetism and neutrals depletion, while the third curve corresponds to high temperature, $T_e = 28\,\mathrm{eV}$, $\beta_n \cong 1$, and high diamagnetism and neutrals depletion. The magnetic field and neutrals are actually expelled by the high beta plasma when neutrals depletion and diamagnetism are high.

This manuscript was accepted by Phys. Plasmas. Click here to see the version of record.

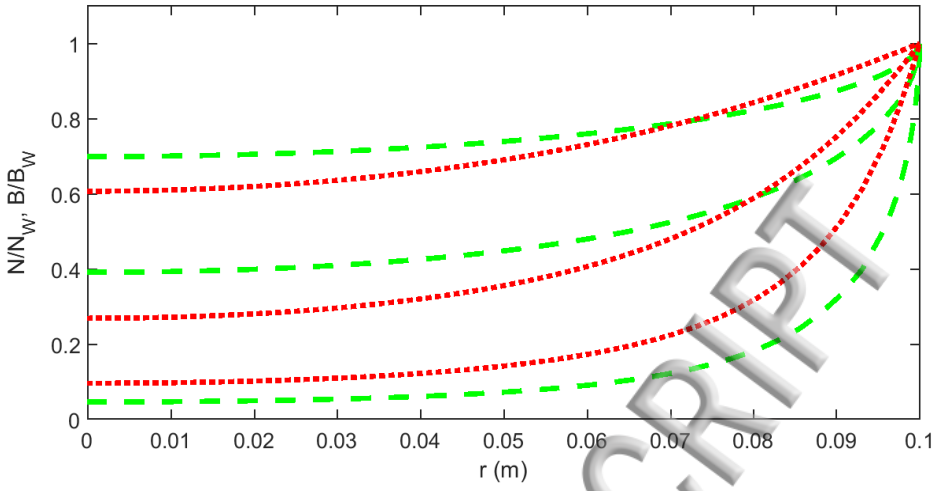

FIG. 12: Case D (helium, $T_g = 300\,\mathrm{K}$, $P_{NW} = 0.5\,\mathrm{Pa}, B_W = 150\,\mathrm{G}, a = 0.1\,\mathrm{m}$). Radial profiles of $\Delta N/N_W$ (dotted, red) and of $\Delta B/B_W$ (dashed, green). Three plasma particle flux densities: 1) $\Gamma_W = 1.7\times10^{22}\,\mathrm{m^{-2}\,s^{-1}}$ ($n_0 = 6\times10^{19}\,\mathrm{m^{-3}}$, $T_e = 4.8\,\mathrm{eV}$), 2) $\Gamma_W = 5.8\times10^{22}\,\mathrm{m^{-2}\,s^{-1}}$ ($n_0 = 7.7\times10^{19}\,\mathrm{m^{-3}}$, $T_e = 6.2\,\mathrm{eV}$), and 3) $\Gamma_W = 1.5\times10^{23}\,\mathrm{m^{-2}\,s^{-1}}$ ($n_0 = 6\times10^{19}\,\mathrm{m^{-3}}$, $T_e = 9.3\,\mathrm{eV}$). $\Delta B/B_W$ is comparable here to $\Delta N/N_W$. Neutrals depletion is comparable to the diamagnetic effect.

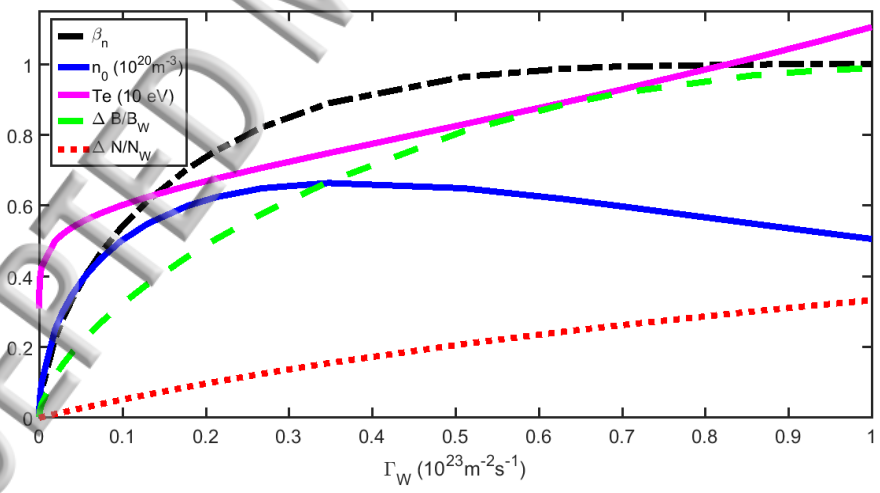

FIG. 13: Case E (helium, $T_g = 1800\,\mathrm{K}$, $P_{NW} = 0.5\,\mathrm{Pa}, B_W = 150\,\mathrm{G}, a = 0.1\,\mathrm{m}$). Electron temperature T_e (solid, magenta), plasma density n_0 (solid, nonmonotonic, blue), plasma beta β_n (dashed - dotted, black), $\Delta B/B_W$ (dashed, green) and $\Delta N/N_W$ (dotted, red) versus plasma flux density Γ_W. Nonmonotonic variation of n_0 due to the increase of cross-field transport with Γ_W. $\Delta B/B_W \gg \Delta N/N_W$.

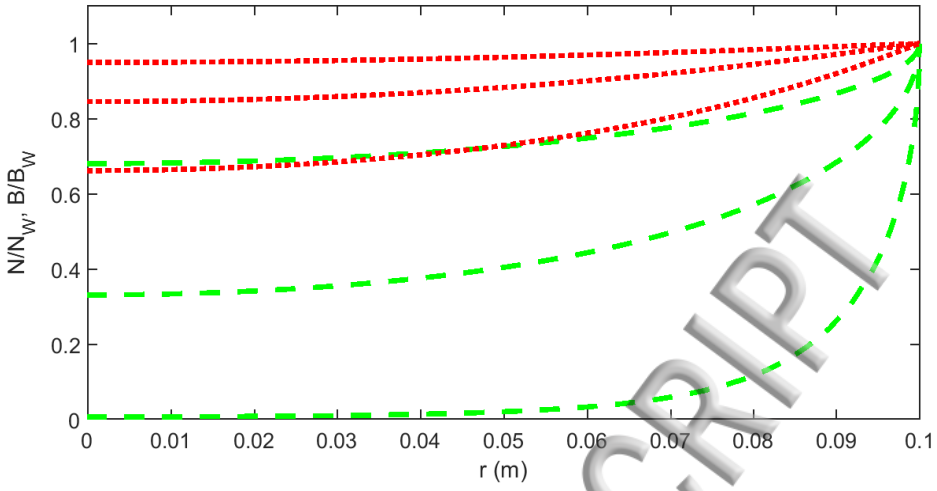

FIG. 14: Case E (helium, $T_g = 1800\,\mathrm{K}$, $P_{NW} = 0.5\,\mathrm{Pa}$, $B_W = 150\,\mathrm{G}$, $a = 0.1\,\mathrm{m}$). Radial profiles of $\Delta N/N_W$ (dotted, red) and of $\Delta B/B_W$ (dashed, green). Three plasma particle flux densities: 1) $\Gamma_W = 9.8 \times 10^{21}\,\mathrm{m^{-2}\,s^{-1}}$ ($n_0 = 5 \times 10^{19}\,\mathrm{m^{-3}}$, $T_e = 6\,\mathrm{eV}$), 2) $\Gamma_W = 3.5 \times 10^{22}\,\mathrm{m^{-2}\,s^{-1}}$ ($n_0 = 6.65 \times 10^{19}\,\mathrm{m^{-3}}$, $T_e = 7.5\,\mathrm{eV}$), and 3) $\Gamma_W = 1.0 \times 10^{23}\,\mathrm{m^{-2}\,s^{-1}}$ ($n_0 = 5 \times 10^{19}\,\mathrm{m^{-3}}$, $T_e = 11.2\,\mathrm{eV}$). $\Delta B/B_W \gg \Delta N/N_W$. The diamagnetic effect is stronger than neutrals depletion.

We should note that when the magnetic field and neutrals are expelled almost completely from the plasma, our model for a magnetized plasma ceases to be valid. Nevertheless, the general behavior is still captured by the model.

In cases D and E the gas is helium. For helium, $\epsilon_i = 24.6\,\mathrm{eV}$, $k_{eN} = 4.54 \times 10^{-14}\,\mathrm{m^3\,s^{-1}}$ (page 62 in [30] and the polarizabilities from https://www.britannica.com/science/noble-gas), and $k_{iN} = 3.15 \times 10^{-16}\,\mathrm{m^3/\,s}$ (estimate from page 77 in [30]). As said above, the magnetic field and the gas pressure are the same for the three cases C, D, and E. The magnetic field is $B_W = 150\,\mathrm{G}$, so that $P_{BW} = 90\,\mathrm{Pa}$, and the helium gas pressure is $P_{NW} = 0.5\,\mathrm{Pa}$, therefore, as in C, $P_B \gg P_N$ and $\beta_N = 0.0056$. The parameter C_1 in the helium discharge is likely to be larger than in the argon discharge, since the ion mass is ten times smaller and k_{iN} is about twice smaller. Therefore, $C_1 \gg 1$ and the plasma pressure in cases D and E is expected to be balanced mostly by the gradient of the magnetic pressure, as it was in case C. The relation $\Delta B/B_W \cong 1 - \sqrt{1-\beta_n}$ also hold in Figs. 11 - 14, that describe the calculations for cases D and E of helium. The parameter C_2 in the helium discharge is also likely to be larger than in the argon discharge, therefore $\Delta B/B_W$ is not likely to be that much smaller than $\Delta N/N_W$, as it was for argon plasma of case C.

The calculations of case D, helium discharge where the gas is at room temperature ($T_g = 300\,\mathrm{K}$), are described in Figures 11 and 12. It is seen in Fig. 11 that, as Γ_W increases, both diamagnetism and neutrals depletion increase; both $\Delta B/B_W$ and $\Delta N/N_W$ increase and eventually reach unity. However, contrary to the argon discharge of case C, in the helium discharge diamagnetism and neutrals depletion are comparable. This is a result of C_2 being about unity. A nonmonotonic dependence of n_0 on Γ_W also occurs for helium. For high Γ_W, as Γ_W increases n_0 decreases while T_e keeps increasing so that β_n gets closer to unity. It is noted that T_e is generally higher in the helium discharge than in the argon discharge because of the higher ionization energy. Indeed, at the limit of negligible diamagnetism and neutrals depletion, $T_e = 2.89\,\mathrm{eV}$ for helium and only $1.9\,\mathrm{eV}$ for argon. However, neutral depletion is larger in argon than in helium, and in order to maintain high ionization despite the lower neutrals density, T_e in argon turns out to be higher.

Figure 12 shows the radial profiles of $\Delta B/B_W$ and of $\Delta N/N_W$ in case D for three plasma particle flux densities, $\Gamma_W = 1.7\times10^{22}\,\mathrm{m^{-2}\,s^{-1}}$, $5.8\times10^{22}\,\mathrm{m^{-2}\,s^{-1}}$, and $1.5\times10^{23}\,\mathrm{m^{-2}\,s^{-1}}$. The plasma densities that correspond to the three flux densities are $n_0 = 6\times10^{19}\,\mathrm{m^{-3}}$, $7.7\times10^{19}\,\mathrm{m^{-3}}$, and again $6\times10^{19}\,\mathrm{m^{-3}}$, respectively. The electron temperatures are $T_e = 4.8\,\mathrm{eV}$, $6.2\,\mathrm{eV}$ and $9.3\,\mathrm{eV}$, respectively. Neutrals depletion is comparable to the diamagnetic effect, $\Delta N/N_W \simeq \Delta B/B_W$. Note that, because of the nonmonotonic dependence of the plasma density, the first curve and the third curve (fourth for n/n_0) are for the same plasma density, $n_0 = 6\times10^{19}\,\mathrm{m^{-3}}$. However, the first curve corresponds to low temperature, $T_e = 4.8\,\mathrm{eV}$, low beta, and low diamagnetism and neutrals depletion, while the third curve corresponds to high temperature, $T_e = 9.3\,\mathrm{eV}$, high beta, and high diamagnetism and neutrals depletion. Such two different steady state plasmas with the same plasma density n_0, that are shown here for case D, were also pointed out in Figs. 8 - 10 for argon (case C). The radial profiles of the plasma density for the three Γ_W are not shown for case D, since they are similar to those shown in Fig. 9 for case C.

Figures 13 and 14 describe the calculations for case E, helium discharge where the gas is at a higher temperature of $1800\,\mathrm{K}$ (and a lower neutral gas density to keep neutrals pressure the same as in cases C and D). From Eq. (27), it is seen that C_2 is larger for a higher gas temperature. This leads, as is shown in the figures, to the diamagnetic effect being more pronounced than in the previous examples of argon and helium at room temperature (cases C and D). Moreover, the diamagnetic effect is actually stronger than neutrals depletion in

this case, $\Delta B/B_W \gg \Delta N/N_W$. It is seen in Fig. 13, similarly to Figs. 8 and 11, that, as Γ_W increases, both diamagnetism and neutrals depletion increase. A nonmonotonic dependence of n_0 on Γ_W also occurs for helium at this higher gas temperature. For high Γ_W, as Γ_W increases n_0 decreases while T_e keeps increasing, and β_n gets closer to unity.

Figure 14 shows the radial profiles of the normalized neutrals density N/N_W and of magnetic field B/B_W in case E. Three plasma particle flux densities are $\Gamma_W = 9.8\times10^{21}\,\mathrm{m^{-2}\,s^{-1}}$, $3.5\times10^{22}\,\mathrm{m^{-2}\,s^{-1}}$ and $1.0\times10^{23}\,\mathrm{m^{-2}\,s^{-1}}$. The corresponding plasma densities are $n_0 = 5\times10^{19}\,\mathrm{m^{-3}}$, $6.65\times10^{19}\,\mathrm{m^{-3}}$ and again $5\times10^{19}\,\mathrm{m^{-3}}$, respectively. The electron temperatures are $T_e = 6\,\mathrm{eV}$, $7.5\,\mathrm{eV}$ and $11\,\mathrm{eV}$. The plasma density profiles are not shown as they are similar to those of case C shown in Fig. 9. Here, $\Delta B/B_W \gg \Delta N/N_W$. The diamagnetic effect is stronger than neutrals depletion.

In this section, a nonmonotonic variation of the plasma density with the plasma particle flux density was demonstrated and explained. Neutrals depletion and diamagnetism were compared for three different cases. A dimensionless parameter was identified that determines which of the two processes is dominant.

VII. THE EFFECT OF THE MAGNETIC FIELD INTENSITY

In this section we examine how diamagnetism and neutrals depletion vary with the intensity of the applied magnetic field. The variation depends on the plasma parameters that are varied or are kept constant. If the plasma density n_0 is kept constant when the magnetic field increases, it is likely that diamagnetism, $\Delta B/B_W$, decreases, because the plasma beta β_n decreases. Neutrals depletion, $\Delta N/N_W$, is also expected to decrease with an increase of the magnetic field in that case, as was explained in [24]. Here, we examine the effect of the variation of the magnetic field in two cases. In the first case, case F, the magnetic field B_W is varied while the maximal plasma density n_0 is indeed kept constant, as was discussed earlier [24]. In the second case, case G, B_W is varied while Γ_W is kept constant. It is shown here that in case G, neutrals depletion, $\Delta N/N_W$, does not decrease with the magnetic field B_W, but rather it is approximately constant. We comment that case G, in which Γ_W is kept constant, corresponds roughly to keeping the deposited power in the plasma constant (this is only approximate, since as T_e changes, the energy cost changes [33, 34], and, therefore, for the same power, Γ_W does change). Our purpose in this section is therefore to demonstrate

numerically the different behavior of neutrals depletion in the two cases, F and G, and to explain the different behavior qualitatively.

The dependence of diamagnetism on the magnetic field intensity was studied experimentally and modelled theoretically in [14]. However, it was difficult in the experiment to vary the magnetic field while keeping either plasma density or plasma particle flux density constant. We study this issue theoretically here.

We choose to model an argon discharge in both cases, F and G. The gas pressure is taken as $P_{NW} = 4\,\mathrm{Pa}$, so that the neutrals pressure is not negligible relative to the magnetic pressure. In addition, following the examples in Figs. 1 - 7 (cases A and B), it is assumed that $T_g = 1800\,\mathrm{K}$. As in all the examples, the radius of the cylindrical tube is $a = 0.1\,\mathrm{m}$.

We start by examining the effect of varying the magnetic field intensity B_W while the maximal plasma density n_0 is kept constant (case F). Figures 15 - 17 show the results of the calculation, in which the plasma maximal density is specified as $n_0 = 1.6 \times 10^{19}\,\mathrm{m}^{-3}$.

Figure 15 shows the electron temperature T_e, the plasma particle flux density Γ_W , the relative change of the magnetic field $\Delta B/B_W$ and the relative change in the neutrals density $\Delta N/N_W$ versus the magnetic field B_W. All these quantities indeed decrease with the magnetic field. In particular, neutrals depletion, $\Delta N/N_W$, decreases with B_W, as claimed in [24].

Some of the dependencies on the magnetic field in Fig. 15 can be understood by examining the governing equations. Because of the decrease of T_e with B_W, Γ_W decreases for a fixed n_0, following Eq. (12). Since Γ decreases, $\Delta N/N_W$ and $\Delta B/B_W$ have to decrease, following Eqs. (11) and (13).

Radial profiles of normalized plasma density n/n_0 are shown in Fig. 16 and of normalized neutrals density N/N_W and magnetic field B/B_W are shown in Fig. 17 for case F. As in Fig. 15, $n_0 = 1.6 \times 10^{19}\,\mathrm{m}^{-3}$. The profiles are for four magnetic field intensities: $B_W = 50\,\mathrm{G}$ ($\Gamma_W = 1.3 \times 10^{22}\,\mathrm{m}^{-2}\,\mathrm{s}^{-1}$, $T_e = 3.3\,\mathrm{eV}$), $60\,\mathrm{G}$ ($\Gamma_W = 7.2 \times 10^{21}\,\mathrm{m}^{-2}\,\mathrm{s}^{-1}$, $T_e = 2.9\,\mathrm{eV}$) , $70\,\mathrm{G}$ ($\Gamma_W = 4.5 \times 10^{21}\,\mathrm{m}^{-2}\,\mathrm{s}^{-1}$, $T_e = 2.7\,\mathrm{eV}$) , and $400\,\mathrm{G}$ ($\Gamma_W = 1.8 \times 10^{20}\,\mathrm{m}^{-2}\,\mathrm{s}^{-1}$, $T_e = 1.7\,\mathrm{eV}$) . As seen in Fig. 17, for a higher B_W, the reductions of both B/B_W and N/N_W are smaller. It is concluded that neutrals depletion indeed decreases with the magnetic field, as claimed in [24].

We note that the case of $B_W = 50\,\mathrm{G}$ is also included in the examples of Figs. 5 -7. We also note that for a lower B_W, in which case neutrals depletion is larger, n/n_0 is slightly

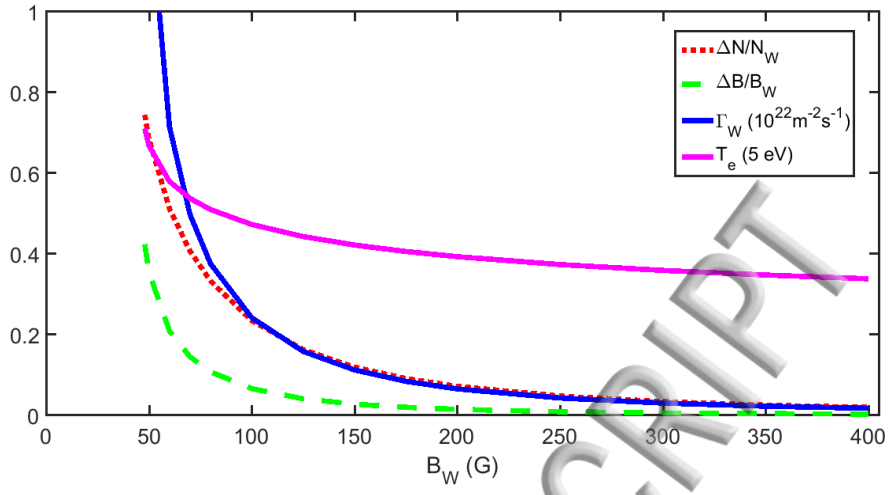

FIG. 15: Case F (argon, $T_g = 1800\,\mathrm{K}$, $P_{NW} = 4\,\mathrm{Pa}$, $B_W = 150\,\mathrm{G}, a = 0.1\,\mathrm{m}$). Plasma density is fixed: $n_0 = 1.6 \times 10^{19}\,\mathrm{m}^{-3}$. Electron temperature T_e (solid, magenta), plasma particle flux density Γ_W (solid, blue), $\Delta B/B_W$ (dashed, green) and $\Delta N/N_W$ (dotted, red) versus the magnetic field B_W. Neutrals depletion decreases with the magnetic field.

more convex. The reasons for n/n_0 becoming more or less convex require further study.

We turn now to examine the effect of varying the magnetic field intensity while the plasma particle flux density at the wall Γ_W is kept constant (case G). Figure 18 shows the electron temperature T_e, the plasma density n_0 the relative changes in the magnetic field $\Delta B/B_W$ and in the neutrals density $\Delta N/N_W$ versus the magnetic field B_W. The plasma particle flux density at the wall is kept constant, $\Gamma_W = 1.3 \times 10^{22}\,\mathrm{m}^{-2}\,\mathrm{s}^{-1}$, while B_W varies. In this case, neutrals depletion hardly varies with the magnetic field. The relative change of the magnetic field $\Delta B/B_W$ and T_e decrease, while n_0 increases approximately linearly with B_W.

The dependence on the magnetic field can be understood by examining the governing equations also here, for case G. From Eq. (11), it is seen that the relative change of the neutrals density is determined by the integral of $m_i k_{iN} \Gamma / T_g$. If Γ_W is kept constant, it is expected that neutrals depletion will be approximately constant as well. The plasma density is determined by Eq. (10), in which we assume that the first term on the RHS is dominant and that electrons collide mostly with ions so that $\nu_e \propto n$. If Γ_W is kept constant, it is seen that $n \propto B$, although diamagnetism and variation of T_e make the dependence less obvious. The numerical calculations include all these effects. Finally, From Eq. (14), we see that $\Delta B/B_W$ varies as the integral of ν_e^{-1} for a constant Γ_W. Since ν_e is roughly proportional to

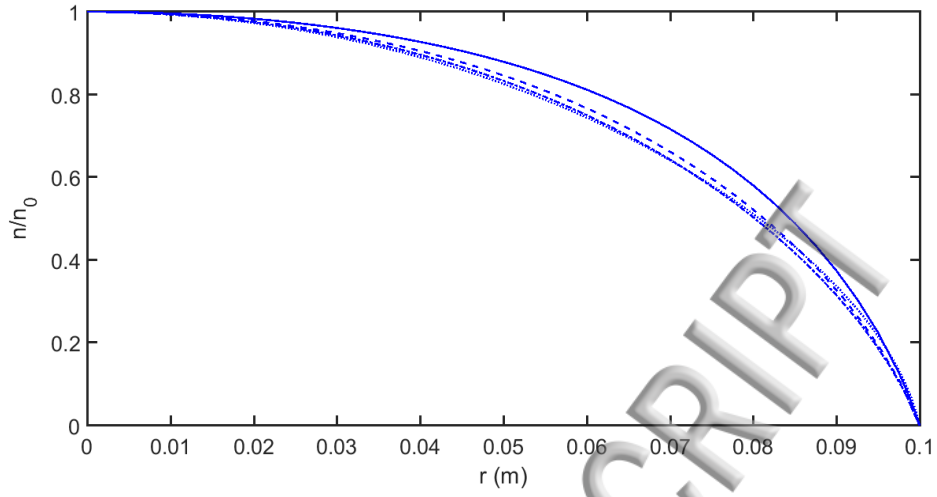

FIG. 16: Case F (argon, $T_g = 1800\,\mathrm{K}$, $P_{NW} = 4\,\mathrm{Pa}$, $B_W = 150\,\mathrm{G}$, $a = 0.1\,\mathrm{m}$). Maximal plasma density is fixed: $n_0 = 1.6 \times 10^{19}\,\mathrm{m}^{-3}$. Radial profiles of normalized plasma density n/n_0 for four magnetic field intensities: 1) $B_W = 50\,\mathrm{G}$ ($\Gamma_W = 1.3 \times 10^{22}\,\mathrm{m}^{-2}\,\mathrm{s}^{-1}$, $T_e = 3.3\,\mathrm{eV}$) - solid, 2) $B_W = 60\,\mathrm{G}$ ($\Gamma_W = 7.2 \times 10^{21}\,\mathrm{m}^{-2}\,\mathrm{s}^{-1}$, $T_e = 2.9\,\mathrm{eV}$) - dashed, 3) $B_W = 70\,\mathrm{G}$ ($\Gamma_W = 4.5 \times 10^{21}\,\mathrm{m}^{-2}\,\mathrm{s}^{-1}$, $T_e = 2.7\,\mathrm{eV}$) - dashed - dotted, and 4) $B_W = 400\,\mathrm{G}$ ($\Gamma_W = 1.8 \times 10^{20}\,\mathrm{m}^{-2}\,\mathrm{s}^{-1}$, $T_e = 1.7\,\mathrm{eV}$) - dotted. The plasma density profile hardly changes with B_W. For a lower B_W, n/n_0 is slightly more convex (for a lower B_W, neutrals depletion is larger - see Fig. 17).

n, it follows that $\Delta B/B_W \propto n^{-1}$. Thus, $n \propto B$ results in $\Delta B/B_W \propto B^{-1}$. Indeed, the the dependence seen in Fig. 18 is roughly $\Delta B/B_W \propto B_W^{-1}$.

Radial profiles of normalized plasma density n/n_0 are shown in Fig. 19, and neutrals density N/N_W and magnetic field B/B_W are shown in Fig. 20, for the same parameters as in Fig. 18 for four magnetic field intensities: $B_W = 10\,\mathrm{G}$ ($n_0 = 4.3 \times 10^{18}\,\mathrm{m}^{-3}$, $T_e = 4.6\,\mathrm{eV}$), $50\,\mathrm{G}$ ($n_0 = 1.6 \times 10^{19}\,\mathrm{m}^{-3}$, $T_e = 3.3\,\mathrm{eV}$) , $150\,\mathrm{G}$ ($n_0 = 5.2 \times 10^{19}\,\mathrm{m}^{-3}$, $T_e = 2.7\,\mathrm{eV}$) and $350\,\mathrm{G}$ ($n_0 = 1.2 \times 10^{20}\,\mathrm{m}^{-3}$, $T_e = 2.3\,\mathrm{eV}$). We note again that the case of $B_W = 50\,\mathrm{G}$ is also included in the examples of Figs. 5 -7. Neutrals depletion is almost constant. The profile of neutral density is almost the same for all magnetic field intensities. The neutrals density is only slightly higher for a higher B_W. Also, the reduction of B/B_W is smaller and n/n_0 is more convex for a higher B_W. As written above, the reasons for n/n_0 becoming more or less convex require further study.

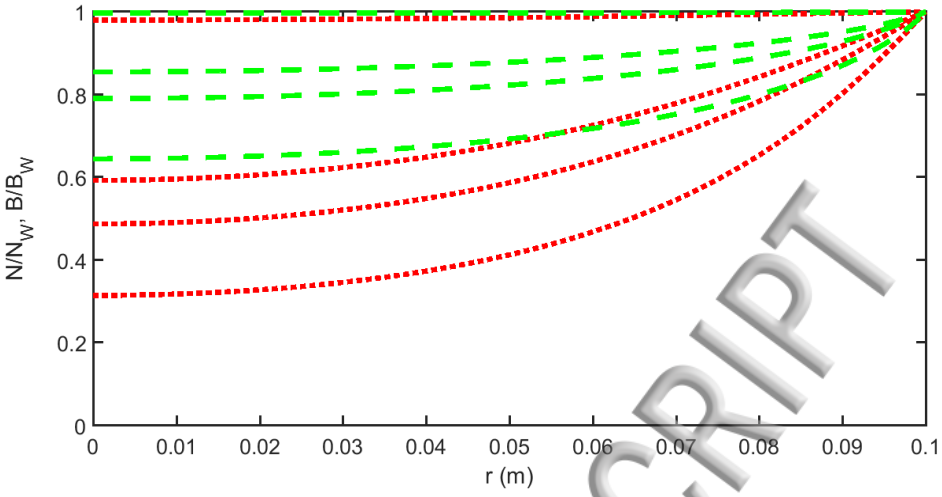

FIG. 17: Case F (argon, $T_g = 1800\,\mathrm{K}$, $P_{NW} = 4\,\mathrm{Pa}$, $B_W = 150\,\mathrm{G}$, $a = 0.1\,\mathrm{m}$). Maximal plasma density is fixed: $n_0 = 1.6\times10^{19}\,\mathrm{m}^{-3}$. Radial profiles of normalized neutrals density N/N_W (dotted, red) and magnetic field B/B_W (dashed, green) for four magnetic field intensities, as in Fig. 16: 1) $B_W = 50\,\mathrm{G}$ ($\Gamma_W = 1.3\times10^{22}\,\mathrm{m}^{-2}\,\mathrm{s}^{-1}$, $T_e = 3.3\,\mathrm{eV}$) , 2) $B_W = 60\,\mathrm{G}$ ($\Gamma_W = 7.2\times10^{21}\,\mathrm{m}^{-2}\,\mathrm{s}^{-1}$, $T_e = 2.9\,\mathrm{eV}$), 3) $B_W = 70\,\mathrm{G}$ ($\Gamma_W = 4.5\times10^{21}\,\mathrm{m}^{-2}\,\mathrm{s}^{-1}$, $T_e = 2.7\,\mathrm{eV}$) , and 4) $B_W = 400\,\mathrm{G}$ ($\Gamma_W = 1.8\times10^{20}\,\mathrm{m}^{-2}\,\mathrm{s}^{-1}$, $T_e = 1.7\,\mathrm{eV}$). For a higher B_W, the decrease of both B/B_W and N/N_W are smaller - diamagnetism and neutrals depletion are smaller.

VIII. CONCLUSIONS

In this paper we have extended our previous study [14] of diamagnetism and neutrals depletion in a magnetized plasma. Both phenomena result from the plasma pressure. We have explored when either magnetic pressure or neutrals pressure balances the plasma pressure. We also determined the condition for either the relative change in the magnetic field (due to diamagnetism) or the relative change in the neutrals density (due to neutrals depletion) to be more pronounced. Two coupling parameters, C_1 and C_2, that indicate which pressure is dominant in the pressure balance and which relative change is more pronounced, were identified. A nonmonotonic dependence of the plasma maximal density on the plasma particle flux density has been identified and explained. Finally, the effect of the magnetic field on neutrals depletion was examined and it was shown that neutral depletion either decreases or does not vary, depending on whether the plasma density of the plasma particle flux density is kept constant while the magnetic field is varied.

This manuscript was accepted by Phys. Plasmas. Click here to see the version of record.

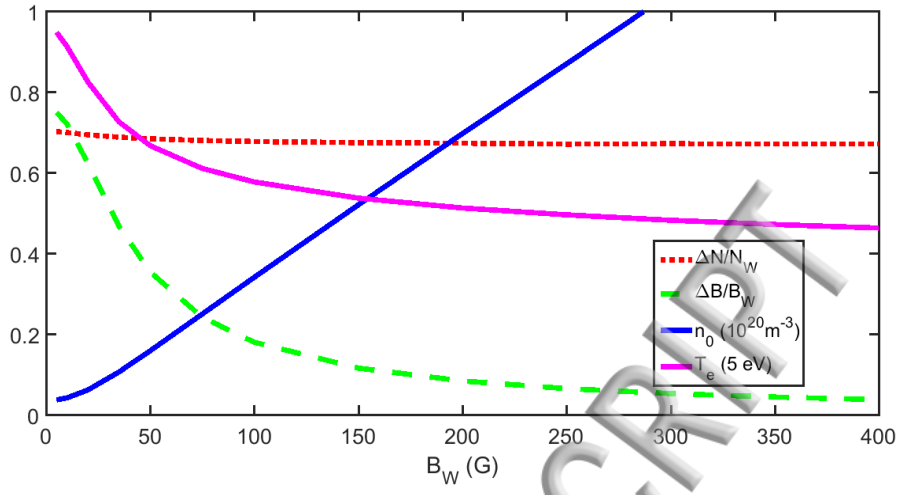

FIG. 18: Case G (argon, $T_g = 1800\,\mathrm{K}$, $P_{NW} = 4\,\mathrm{Pa}, B_W = 150\,\mathrm{G}, a = 0.1\,\mathrm{m}$). Plasma particle flux density is fixed: $\Gamma_W = 1.3 \times 10^{22}\,\mathrm{m}^{-2}\,\mathrm{s}^{-1}$. Electron temperature T_e (solid, magenta), plasma particle flux density Γ_W (solid, blue), $\Delta B/B_W$ (dashed, green) and $\Delta N/N_W$ (dotted, red) versus the magnetic field B_W. Neutrals depletion hardly varies with the magnetic field.

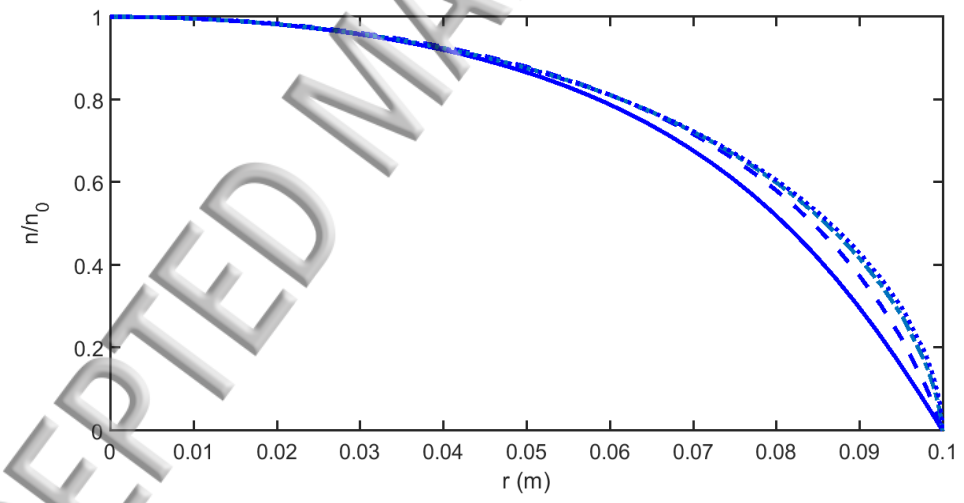

FIG. 19: Case G (argon, $T_g = 1800\,\mathrm{K}$, $P_{NW} = 4\,\mathrm{Pa}, B_W = 150\,\mathrm{G}, a = 0.1\,\mathrm{m}$). Plasma particle flux density is fixed: $\Gamma_W = 1.3 \times 10^{22}\,\mathrm{m}^{-2}\,\mathrm{s}^{-1}$. Radial profiles of normalized plasma density n/n_0 for four magnetic field intensities: 1) $B_W = 10\,\mathrm{G}$ ($n_0 = 4.3 \times 10^{18}\,\mathrm{m}^{-3}$, $T_e = 4.6\,\mathrm{eV}$) - solid, 2) $B_W = 50\,\mathrm{G}$ ($n_0 = 1.6 \times 10^{19}\,\mathrm{m}^{-3}$, $T_e = 3.3\,\mathrm{eV}$) - dashed, 3) $B_W = 150\,\mathrm{G}$ ($n_0 = 5.2 \times 10^{19}\,\mathrm{m}^{-3}$, $T_e = 2.7\,\mathrm{eV}$) - dashed - dotted, and 4) $B_W = 350\,\mathrm{G}$ ($n_0 = 1.2 \times 10^{20}\,\mathrm{m}^{-3}$, $T_e = 2.3\,\mathrm{eV}$) - dotted. The plasma density profile hardly changes with B_W. For a higher B_W, n/n_0 is slightly more convex.

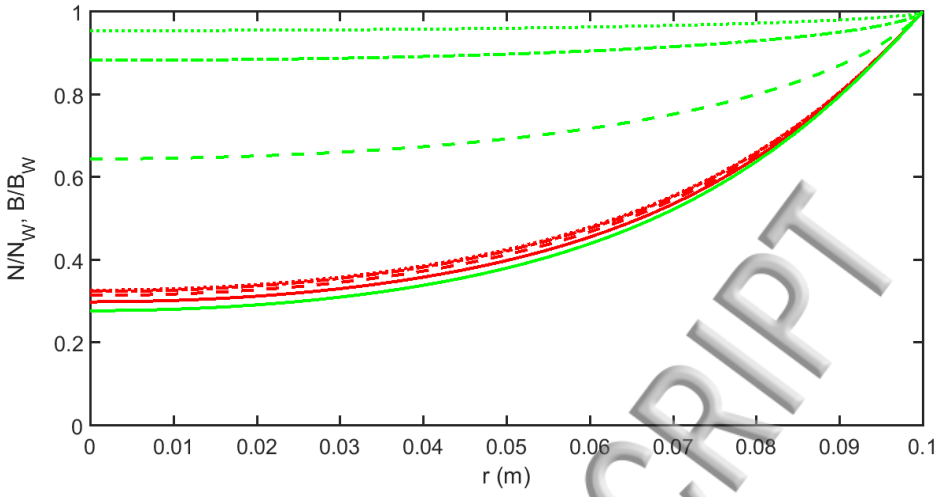

FIG. 20: Case G (argon, $T_g = 1800\,\mathrm{K}$, $P_{NW} = 4\,\mathrm{Pa}$, $B_W = 150\,\mathrm{G}$, $a = 0.1\,\mathrm{m}$). Plasma particle flux density is fixed: $\Gamma_W = 1.3 \times 10^{22}\,\mathrm{m^{-2}\,s^{-1}}$. Radial profiles of normalized neutrals density N/N_W (dotted, red) and magnetic field B/B_W (dashed, green) for four magnetic field intensities, as in Fig. 19: 1) $B_W = 10\,\mathrm{G}$ ($n_0 = 4.3 \times 10^{18}\,\mathrm{m^{-3}}$, $T_e = 4.6\,\mathrm{eV}$) , 2) $50\,\mathrm{G}$ ($n_0 = 1.6 \times 10^{19}\,\mathrm{m^{-3}}$, $T_e = 3.3\,\mathrm{eV}$) , 3) $150\,\mathrm{G}$ ($n_0 = 5.2 \times 10^{19}\,\mathrm{m^{-3}}$, $T_e = 2.7\,\mathrm{eV}$), and 4) $350\,\mathrm{G}$ ($n_0 = 1.2 \times 10^{20}\,\mathrm{m^{-3}}$, $T_e = 2.3\,\mathrm{eV}$). For a higher B_W, the decrease of B/B_W is smaller (smaller diamagnetism). N/N_W hardly varies with B_W, and the decrease of N/N_W is very slightly smaller (a slightly smaller neutrals depletion) when B_W is increased.

Various assumptions have been made in formulating the model. For various cases, it is needed to relax some of these assumptions. As an example, when neutral depletion is intense, neutrals density may become smaller than the plasma density and the model should be modified to account for that.

We should note that for certain applications, it is important that plasma mostly flow axially along magnetic field lines. This is true for helicons used in electric propulsion, for example [35]. Such cylindrical plasmas with flow mostly axial should be modeled differently.

IX. ACKNOWLEDGMENTS

The authors are grateful to Dr. D. Kuwahara for useful discussions. A. F. was supported by the Japan Society for the Promotion of Science (JSPS) Invitation Fellowship under Contract No. S14033, and by the Israel Science Foundation, Grants no. 765/11 and 1581/16.

S.S. has been partly supported by NIFS budget code NIFS17KBAP035.

[1] K. Miyamoto, "Plasma Physics for Nuclear Fusion," (The MIT Press, Cambridge, 1979).

[2] D. Leneman, W. Gekelman, and J. Maggs, Phys. Rev. Lett. **82**, 2673 (1999).

[3] M. Ichimura, M. Inutake, T. Katanuma, N. Hino, H. Hojo, K. Ishii, T. Tamano, and S. Miyoshi, Phys. Rev. Lett. **70**, 2734 (1993).

[4] T. Tsurutani, G. S. Lakhina, O. P. Verkhoglyadova, E. Echer, F. L. Guamieri, Y. Narita, and D. O. Constantinescu, J. Geophys. Res. **116**, A02103 (2011).

[5] R.W. Boswell, Phys. Lett. **33A**, 457 (1970).

[6] E. Scime, P. A. Keiter, M. M. Balkey, R. F. Boivin, J. L. Kline, and M. Blackburn, Phys. Plasmas **7**, 2157 (2000).

[7] R. Stenzel and J. M. Urrutia, Phys. Plasmas **7**, 4450 (2000).

[8] C. S. Corr and R. W. Boswell, Phys. Plasmas **14**, 122503 (2007).

[9] S. Shinohara, T. Motomura, K. Tanaka, T. Tanikawa, and K. P. Shamrai, Plasma Sources Sci. Technol. **19**, 034018 (2010).

[10] B. R. Roberson, R. Winglee, and J. Prager, Phys. Plasmas **18**, 053505 (2011).

[11] K. Takahashi, C. Charles, and R. W. Boswell, Phys. Rev. Lett. **110**, 195003 (2013).

[12] K. Takahashi, A. Chiba, A. Komuro and A. Ando, Plasma Sources Sci. Technol. **25**, 055011 (2016).

[13] K. Takahashi and A. Ando, Phys. Rev. Lett. **118**, 225002 (2017).

[14] S. Shinohara, D. Kuwahara, K. Yano, and A. Fruchtman, Phys. Plasmas **23**, 122108 (2016).

[15] S. Shinohara, T. Hada, T. Motomura, K. Tanaka, T. Tanikawa, K. Toki, Y. Tanaka, and K. P. Shamrai, Phys. Plasmas **16**, 057104 (2009).

[16] S. Shinohara, S. Takechi, and Y. Kawai, Jpn. J. Appl. Phys. **35**, 4503 (1996).

[17] A. Caruso and A. Cavaliere, Brit. J. Appl. Phys. **15**, 1021 (1964).

[18] H.-B. Valentini, Beitr. Plasmaphysik **11**, 483 (1971) (in German, English Abstract).

[19] P. C. Stangeby and J. E. Allen, J. Phys. A: Gen. Phys. **4,** 108 **(**1971); J. Phys. D: Appl. Phys. **6**, 1373 (1973).

[20] J. Gilland, R. Breun, and N. Hershkowitz, Plasma Sources Sci. Technol. **7**, 416 (1998).

[21] S. Cho, Phys. Plasmas **6**, 359 (1999).

[22] A. Fruchtman, G. Makrinich, P. Chabert, and J. M. Rax, Phys. Rev. Lett. **95**, 115002 (2005).

[23] A. Fruchtman, Plasma Sources Sci. Technol. **18**, 025033 (2009).

[24] L. Liard, J.-L. Raimbault, and P. Chabert, Phys. Plasmas **16**, 053507 (2009).

[25] A. Simon, Phys. Rev. **98**, 317 (1955).

[26] A. Fruchtman, G. Makrinich, and J. Ashkenazy, Plasma Sources Sci. Technol. **14**, 152 (2005).

[27] N. Sternberg, V. Godyak, and D. Hoffman, Phys. Plasmas **13**, 063511 (2006).

[28] T. M. G. Zimmermann, M. Coppins, and J. E. Allen, Phys. Plasmas **16**, 043501 (2009).

[29] E. Ahedo, Phys. Plasmas **16**, 113503 (2009).

[30] M. A. Lieberman and A. J. and Lichtenberg, *Principles of Plasma Discharges and Materials Processing*, Second Edition, (Wiley, New York, 2005).

[31] A. Fruchtman, Plasma Sources Sci. Technol. 17, 024016 (2008).

[32] L. Liard, J.-L. Raimbault, J.-M. Rax, and P. Chabert, J. Phys. D: Appl. Phys. **40**, 5192(2007).

[33] J. T. Gudmundsson, Report RH-21-2002, Science Institute, Univ. Iceland, Reykjavik, Iceland (2002).

[34] A. T. Hjartarson, E. G. Thorsteinsson, and J. T. Gudmundsson, Plasma Sources Science and Technology **19**, 065008 (2010).

[35] C. Charles, Journal of Physics D: Applied Physics **42**, 163001 (2009).

Figure Captions

Fig. 1. Case A (argon, $T_g = 300\,\mathrm{K}, P_{NW} = 4\,\mathrm{Pa}, B_W = 50\,\mathrm{G}, a = 0.1\,\mathrm{m}$). Normalized plasma density profiles n/n_0 for three plasma densities, 1) $n_0 = 10^{18}\,\mathrm{m}^{-3}$, 2) $n_0 = 6.5 \times 10^{18}\,\mathrm{m}^{-3}$, and 3) $n_0 = 1.3 \times 10^{19}\,\mathrm{m}^{-3}$. For the lowest density, denoted as 1 (blue - online), the profile coincides with the linear solution (dashed line) [Eq. (30)]. As the plasma density is higher, the profile is more convex.

Fig. 2. Case A (argon, $T_g = 300\,\mathrm{K}, P_{NW} = 4\,\mathrm{Pa}, B_W = 50\,\mathrm{G}, a = 0.1\,\mathrm{m}$). Normalized neutrals density profiles (N/N_W) due to neutrals depletion for the three plasma densities as in Fig. 1. The dotted lines show the approximated expression, Eq. (31), where l1, l2 and l3 denote neutrals density profiles for the three plasma densities in an increasing order. The higher n_0 is, the lower is the neutrals density.

Fig. 3. Case A (argon, $T_g = 300\,\mathrm{K}, P_{NW} = 4\,\mathrm{Pa}, B_W = 50\,\mathrm{G}, a = 0.1\,\mathrm{m}$). Normalized magnetic field profiles (B/B_W) due to diamagnetic currents for the three plasma densities as in Fig. 1. The dotted lines show the approximated expression, Eq. (32), where l1, l2 and l3 denote magnetic field profiles for the three plasma densities in an increasing order. The higher n_0 is, the lower is the magnetic field.

Fig. 4. Case A (argon, $T_g = 300\,\mathrm{K}, P_{NW} = 4\,\mathrm{Pa}, B_W = 50\,\mathrm{G}, a = 0.1\,\mathrm{m}$). Magnetic pressure P_B, Neutrals pressure P_N and plasma pressure P_n for $n_0 = 1.3 \times 10^{19}\,\mathrm{m}^{-3}$. Neutrals pressure is dominant over magnetic pressure: $\Delta P_N > \Delta P_B$.

Fig. 5. Case B (argon, $T_g = 1800\,\mathrm{K}, P_{NW} = 4\,\mathrm{Pa}, B_W = 50\,\mathrm{G}, a = 0.1\,\mathrm{m}$). Normalized neutrals density profiles (N/N_W) due to neutrals depletion for three plasma densities, 1) $n_0 = 10^{18}\,\mathrm{m}^{-3}$, 2) $n_0 = 8 \times 10^{18}\,\mathrm{m}^{-3}$, and 3) $n_0 = 1.6 \times 10^{19}\,\mathrm{m}^{-3}$. As in Fig. 2, the dotted lines show the approximated expression, Eq. (31), where l1, l2 and l3 denote neutrals density profiles for the three plasma densities in an increasing order. The higher n_0 is, the lower is the neutrals density.

Fig. 6. Case B (argon, $T_g = 1800\,\mathrm{K}, P_{NW} = 4\,\mathrm{Pa}, B_W = 50\,\mathrm{G}, a = 0.1\,\mathrm{m}$). Normalized magnetic field profiles (B/B_W) due to diamagnetic currents for the three argon plasma densities and the same parameters as in Fig. 5. As in Fig. 3, the dotted lines show the approximated expression, Eq. (32), where l1, l2 and l3 denote magnetic field profiles for the three plasma densities in an increasing order. The higher n_0 is, the lower is the magnetic field.

Fig. 7. Case B (argon, $T_g = 1800\,\mathrm{K}, P_{NW} = 4\,\mathrm{Pa}, B_W = 50\,\mathrm{G}, a = 0.1\,\mathrm{m}$). Magnetic pressure P_B, Neutrals pressure P_N and plasma pressure P_n for $n_0 = 1.6 \times 10^{19}\,\mathrm{m}^{-3}$. The same magnetic pressure and neutrals pressure at the wall as in Fig. 4, but magnetic pressure is dominant here over neutrals pressure, $\Delta P_B > \Delta P_N$.

Fig. 8. Case C (argon, $T_g = 300\,\mathrm{K}$, $P_{NW} = 0.5\,\mathrm{Pa}$, $B_W = 150\,\mathrm{G}, a = 0.1\,\mathrm{m}$). Electron temperature T_e (solid, magenta), plasma density n_0 (solid, nonmonotonic, blue), plasma beta β_n (dashed - dotted, black), $\Delta B/B_W$ (dashed, green) and $\Delta N/N_W$ (dotted, red) versus plasma flux density Γ_W. Nonmonotonic variation of n_0 due to the increase of cross-field transport with Γ_W; $\Delta N/N_W \gg \Delta B/B_W$.

Fig. 9. Case C (argon, $T_g = 300\,\mathrm{K}$, $P_{NW} = 0.5\,\mathrm{Pa}$, $B_W = 150\,\mathrm{G}, a = 0.1\,\mathrm{m}$). Radial profiles of plasma density n/n_0 for various plasma particle flux densities Γ_W. The most concave profile is at the linear limit: 1) $\Gamma_W = 5 \times 10^{19}\,\mathrm{m}^{-2}\,\mathrm{s}^{-1}$ ($n_0 = 2.5 \times 10^{18}\,\mathrm{m}^{-3}$, $T_e = 1.9\,\mathrm{eV}$, negligible diamagnetism and neutrals depletion) - solid. The other three profiles are for : 2) $\Gamma_W = 2 \times 10^{21}\,\mathrm{m}^{-2}\,\mathrm{s}^{-1}$ ($n_0 = 2 \times 10^{19}\,\mathrm{m}^{-3}$, $T_e = 2.5\,\mathrm{eV}$) - dashed, 3) $\Gamma_W = 6 \times 10^{22}\,\mathrm{m}^{-2}\,\mathrm{s}^{-1}$ ($n_0 = 4.55 \times 10^{19}\,\mathrm{m}^{-3}$, $T_e = 9.6\,\mathrm{eV}$) - dashed-dotted, and 4) $\Gamma_W = 1 \times 10^{23}\,\mathrm{m}^{-2}\,\mathrm{s}^{-1}$ ($n_0 = 2 \times 10^{19}\,\mathrm{m}^{-3}$, $T_e = 28\,\mathrm{eV}$) - dotted. As Γ_W is larger, the plasma density profile is more convex.

Fig. 10. Case C (argon, $T_g = 300\,\mathrm{K}$, $P_{NW} = 0.5\,\mathrm{Pa}$, $B_W = 150\,\mathrm{G}, a = 0.1\,\mathrm{m}$). Radial profiles of $\Delta N/N_W$ (dotted, red) and of $\Delta B/B_W$ (dashed, green) for 1) $\Gamma_W = 2 \times 10^{21}\,\mathrm{m}^{-2}\,\mathrm{s}^{-1}$ ($n_0 = 2 \times 10^{19}\,\mathrm{m}^{-3}$, $T_e = 2.5\,\mathrm{eV}$), 2) $6 \times 10^{22}\,\mathrm{m}^{-2}\,\mathrm{s}^{-1}$ ($n_0 = 4.55 \times 10^{19}\,\mathrm{m}^{-3}$, $T_e = 9.6\,\mathrm{eV}$), and 3) $1 \times 10^{23}\,\mathrm{m}^{-2}\,\mathrm{s}^{-1}$ ($n_0 = 2 \times 10^{19}\,\mathrm{m}^{-3}$, $T_e = 28\,\mathrm{eV}$). As Γ_W is larger, $\Delta N/N_W$ and $\Delta B/B_W$ are larger. $\Delta N/N_W \gg \Delta B/B_W$, except for the highest Γ_W when both $\Delta N/N_W$ and $\Delta B/B_W$ are close to unity. Neutrals depletion is much more pronounced than the diamagnetic effect.

Fig. 11. Case D (helium, $T_g = 300\,\mathrm{K}$, $P_{NW} = 0.5\,\mathrm{Pa}, B_W = 150\,\mathrm{G}, a = 0.1\,\mathrm{m}$). Electron temperature T_e (solid, magenta), plasma density n_0 (solid, nonmonotonic, blue), plasma beta β_n (dashed - dotted, black), $\Delta B/B_W$ (dashed, green) and $\Delta N/N_W$ (dotted, red) versus plasma flux density Γ_W. Nonmonotonic variation of n_0 due to the increase of cross-field transport with Γ_W; $\Delta N/N_W$ and $\Delta B/B_W$ are similar in magnitude.

Fig. 12. Case D (helium, $T_g = 300\,\mathrm{K}$, $P_{NW} = 0.5\,\mathrm{Pa}, B_W = 150\,\mathrm{G}, a = 0.1\,\mathrm{m}$). Radial profiles of $\Delta N/N_W$ (dotted, red) and of $\Delta B/B_W$ (dashed, green). Three plasma particle flux densities: 1) $\Gamma_W = 1.7 \times 10^{22}\,\mathrm{m}^{-2}\,\mathrm{s}^{-1}$ ($n_0 = 6 \times 10^{19}\,\mathrm{m}^{-3}$, $T_e = 4.8\,\mathrm{eV}$), 2) $\Gamma_W =$

$5.8 \times 10^{22}\,\mathrm{m^{-2}\,s^{-1}}$ ($n_0 = 7.7 \times 10^{19}\,\mathrm{m^{-3}}$, $T_e = 6.2\,\mathrm{eV}$), and 3) $\Gamma_W = 1.5 \times 10^{23}\,\mathrm{m^{-2}\,s^{-1}}$ ($n_0 = 6 \times 10^{19}\,\mathrm{m^{-3}}$, $T_e = 9.3\,\mathrm{eV}$). $\Delta B/B_W$ is comparable here to $\Delta N/N_W$. Neutrals depletion is comparable to the diamagnetic effect.

Fig. 13. Case E (helium, $T_g = 1800\,\mathrm{K}$, $P_{NW} = 0.5\,\mathrm{Pa}$, $B_W = 150\,\mathrm{G}$, $a = 0.1\,\mathrm{m}$). Electron temperature T_e (solid, magenta), plasma density n_0 (solid, nonmonotonic, blue), plasma beta β_n (dashed - dotted, black), $\Delta B/B_W$ (dashed, green) and $\Delta N/N_W$ (dotted, red) versus plasma flux density Γ_W. Nonmonotonic variation of n_0 due to the increase of cross-field transport with Γ_W. $\Delta B/B_W \gg \Delta N/N_W$.

Fig. 14. Case E (helium, $T_g = 1800\,\mathrm{K}$, $P_{NW} = 0.5\,\mathrm{Pa}$, $B_W = 150\,\mathrm{G}$, $a = 0.1\,\mathrm{m}$). Radial profiles of $\Delta N/N_W$ (dotted, red) and of $\Delta B/B_W$ (dashed, green). Three plasma particle flux densities: 1) $\Gamma_W = 9.8 \times 10^{21}\,\mathrm{m^{-2}\,s^{-1}}$ ($n_0 = 5 \times 10^{19}\,\mathrm{m^{-3}}$, $T_e = 6\,\mathrm{eV}$), 2) $\Gamma_W = 3.5 \times 10^{22}\,\mathrm{m^{-2}\,s^{-1}}$ ($n_0 = 6.65 \times 10^{19}\,\mathrm{m^{-3}}$, $T_e = 7.5\,\mathrm{eV}$), and 3) $\Gamma_W = 1.0 \times 10^{23}\,\mathrm{m^{-2}\,s^{-1}}$ ($n_0 = 5 \times 10^{19}\,\mathrm{m^{-3}}$, $T_e = 11.2\,\mathrm{eV}$). $\Delta B/B_W \gg \Delta N/N_W$. The diamagnetic effect is stronger than neutrals depletion.

Fig. 15. Case F (argon, $T_g = 1800\,\mathrm{K}$, $P_{NW} = 4\,\mathrm{Pa}$, $B_W = 150\,\mathrm{G}$, $a = 0.1\,\mathrm{m}$). Plasma density is fixed: $n_0 = 1.6 \times 10^{19}\,\mathrm{m^{-3}}$. Electron temperature T_e (solid, magenta), plasma particle flux density Γ_W (solid, blue), $\Delta B/B_W$ (dashed, green) and $\Delta N/N_W$ (dotted, red) versus the magnetic field B_W. Neutrals depletion decreases with the magnetic field.

Fig. 16. Case F (argon, $T_g = 1800\,\mathrm{K}$, $P_{NW} = 4\,\mathrm{Pa}$, $B_W = 150\,\mathrm{G}$, $a = 0.1\,\mathrm{m}$). Maximal plasma density is fixed: $n_0 = 1.6 \times 10^{19}\,\mathrm{m^{-3}}$. Radial profiles of normalized plasma density n/n_0 for four magnetic field intensities: 1) $B_W = 50\,\mathrm{G}$ ($\Gamma_W = 1.3 \times 10^{22}\,\mathrm{m^{-2}\,s^{-1}}$, $T_e = 3.3\,\mathrm{eV}$) - solid, 2) $B_W = 60\,\mathrm{G}$ ($\Gamma_W = 7.2 \times 10^{21}\,\mathrm{m^{-2}\,s^{-1}}$, $T_e = 2.9\,\mathrm{eV}$) - dashed, 3) $B_W = 70\,\mathrm{G}$ ($\Gamma_W = 4.5 \times 10^{21}\,\mathrm{m^{-2}\,s^{-1}}$, $T_e = 2.7\,\mathrm{eV}$) - dashed - dotted, and 4) $B_W = 400\,\mathrm{G}$ ($\Gamma_W = 1.8 \times 10^{20}\,\mathrm{m^{-2}\,s^{-1}}$, $T_e = 1.7\,\mathrm{eV}$) - dotted. The plasma density profile hardly changes with B_W. For a lower B_W, n/n_0 is slightly more convex (for a lower B_W, neutrals depletion is larger - see Fig. 17).

Fig. 17. Case F (argon, $T_g = 1800\,\mathrm{K}$, $P_{NW} = 4\,\mathrm{Pa}$, $B_W = 150\,\mathrm{G}$, $a = 0.1\,\mathrm{m}$). Maximal plasma density is fixed: $n_0 = 1.6 \times 10^{19}\,\mathrm{m^{-3}}$. Radial profiles of normalized neutrals density N/N_W (dotted, red) and magnetic field B/B_W (dashed, green) for four magnetic field intensities, as in Fig. 16: 1) $B_W = 50\,\mathrm{G}$ ($\Gamma_W = 1.3 \times 10^{22}\,\mathrm{m^{-2}\,s^{-1}}$, $T_e = 3.3\,\mathrm{eV}$) , 2) $B_W = 60\,\mathrm{G}$ ($\Gamma_W = 7.2 \times 10^{21}\,\mathrm{m^{-2}\,s^{-1}}$, $T_e = 2.9\,\mathrm{eV}$), 3) $B_W = 70\,\mathrm{G}$ ($\Gamma_W = 4.5 \times 10^{21}\,\mathrm{m^{-2}\,s^{-1}}$, $T_e = 2.7\,\mathrm{eV}$) , and 4) $B_W = 400\,\mathrm{G}$ ($\Gamma_W = 1.8 \times 10^{20}\,\mathrm{m^{-2}\,s^{-1}}$, $T_e = 1.7\,\mathrm{eV}$). For a higher B_W,

ing decrease of both B/B_W and N/N_W are smaller - diamagnetism and neutrals depletion are smaller.

Fig. 18. Case G (argon, $T_g = 1800\,\mathrm{K}$, $P_{NW} = 4\,\mathrm{Pa}$, $B_W = 150\,\mathrm{G}$, $a = 0.1\,\mathrm{m}$). Plasma particle flux density is fixed: $\Gamma_W = 1.3 \times 10^{22}\,\mathrm{m^{-2}\,s^{-1}}$. Electron temperature T_e (solid, magenta), plasma particle flux density Γ_W (solid, blue), $\Delta B/B_W$ (dashed, green) and $\Delta N/N_W$ (dotted, red) versus the magnetic field B_W. Neutrals depletion hardly varies with the magnetic field.

Fig. 19. Case G (argon, $T_g = 1800\,\mathrm{K}$, $P_{NW} = 4\,\mathrm{Pa}$, $B_W = 150\,\mathrm{G}$, $a = 0.1\,\mathrm{m}$). Plasma particle flux density is fixed: $\Gamma_W = 1.3 \times 10^{22}\,\mathrm{m^{-2}\,s^{-1}}$. Radial profiles of normalized plasma density n/n_0 for four magnetic field intensities: 1) $B_W = 10\,\mathrm{G}$ ($n_0 = 4.3 \times 10^{18}\,\mathrm{m^{-3}}$, $T_e = 4.6\,\mathrm{eV}$) - solid, 2) $B_W = 50\,\mathrm{G}$ ($n_0 = 1.6 \times 10^{19}\,\mathrm{m^{-3}}$, $T_e = 3.3\,\mathrm{eV}$) - dashed, 3) $B_W = 150\,\mathrm{G}$ ($n_0 = 5.2 \times 10^{19}\,\mathrm{m^{-3}}$, $T_e = 2.7\,\mathrm{eV}$) - dashed - dotted, and 4) $B_W = 350\,\mathrm{G}$ ($n_0 = 1.2 \times 10^{20}\,\mathrm{m^{-3}}$, $T_e = 2.3\,\mathrm{eV}$) - dotted. The plasma density profile hardly changes with B_W. For a higher B_W, n/n_0 is slightly more convex.

Fig. 20. Case G (argon, $T_g = 1800\,\mathrm{K}$, $P_{NW} = 4\,\mathrm{Pa}$, $B_W = 150\,\mathrm{G}$, $a = 0.1\,\mathrm{m}$). Plasma particle flux density is fixed: $\Gamma_W = 1.3 \times 10^{22}\,\mathrm{m^{-2}\,s^{-1}}$. Radial profiles of normalized neutrals density N/N_W (dotted, red) and magnetic field B/B_W (dashed, green) for four magnetic field intensities, as in Fig. 19: 1) $B_W = 10\,\mathrm{G}$ ($n_0 = 4.3 \times 10^{18}\,\mathrm{m^{-3}}$, $T_e = 4.6\,\mathrm{eV}$) , 2) $50\,\mathrm{G}$ ($n_0 = 1.6 \times 10^{19}\,\mathrm{m^{-3}}$, $T_e = 3.3\,\mathrm{eV}$), 3) $150\,\mathrm{G}$ ($n_0 = 5.2 \times 10^{19}\,\mathrm{m^{-3}}$, $T_e = 2.7\,\mathrm{eV}$), and 4) $350\,\mathrm{G}$ ($n_0 = 1.2 \times 10^{20}\,\mathrm{m^{-3}}$, $T_e = 2.3\,\mathrm{eV}$). For a higher B_W, the decrease of B/B_W is smaller (smaller diamagnetism). N/N_W hardly varies with B_W, and the decrease of N/N_W is very slightly smaller (a slightly smaller neutrals depletion) when B_W is increased.